Testing of Precast Bridge Bent Cap Connection Details

by

Güçlü Sümen, B.S.C.E

Thesis

Presented to the Faculty of the Graduate School of

The University of Texas at Austin

in Partial Fulfillment

of the Requirements

for the Degree of

Master of Science in Engineering

The University of Texas at Austin

December 1999

Testing of Precast Bridge Bent Cap Connection Details

Approved by
Supervising Committee:

Supervisor: M.E. Kreger

S.L. Wood

For my parents for their love and support

Acknowledgements

My sincere appreciation is given to my supervising professors, Dr. Michael E. Kreger, and Dr. Sharon L. Wood for their support and guidance.

I am grateful to Eric E. Matsumoto for his efforts during the project. My thanks are also extended to Ferguson Structural Engineering Laboratory staff who cooperated to make this project possible.

Finally, I would like to express my deepest gratitude to my family for their support, love and encouragement.

Güçlü Sümen
December 1999
Austin, Texas

Testing Precast Bridge Bent Cap Connection Details

by

Güçlü Sümen, M.S.E.

The University of Texas at Austin, 1999

Supervisor: Michael E. Kreger

Texas Department of Transportation (TxDOT) has been utilizing precast bent-caps in recent bridge projects, as an alternative solution for cast-in-place type construction. Although precast bent-caps look like to pace construction process on site, there are several challenges need to be carefully examined. These include economy, ease of erection, durability, and load transfer issues. To address the concerns, four precast bent-caps with single line grout pocket, double line grout pocket, vertical duct, and bolted type connection details were designed and tested.

Table of Contents

CHAPTER 1

INTRODUCTION

1.1 BACKGROUND

The Texas Department of Transportation (TxDOT) has been investigating alternative techniques for bridge construction in urban areas to reduce the costs associated with and impact of traffic control and disrupted traffic flow. One alternative is the use of precast rather than cast-in-place construction. Precast superstructures such as precast, prestressed beams and panels are commonly used in bridge construction. Consistent, efficient production of high-quality products, reduction in construction time, and minimization of environmental impact associated with construction are all common benefits resulting from use of precast members. As a result, TxDOT is interested in using precast bent-caps in bridge substructures. Precast bent-caps have been used in two TxDOT projects and were shown to be cost-effective.

Although precast bent-caps appear to provide an immediate solution for expediting urban bridge construction, there are a number of details that need to be addressed. Using precast bent-caps requires tighter tolerances than are currently required by cast-in-place construction, so new construction techniques or processes will likely need to be developed. Constructable joint details between the cap and cast-in-place column or pile must be developed. Additionally,

uncertainty exists regarding the ability of the precast connection to transfer the necessary loads.

Bent-caps support the longitudinal girders in the superstructure. Girders rest on neoprene or steel bearings that are located on the top surface of the bent-caps. Bent-caps also contribute to the vertical and longitudinal stability of a bridge. If connected properly, a bent-cap and columns act as a moment-resisting frame under lateral load, such as wind. Under longitudinal forces, a bent-cap transfers shear to the columns.

A preliminary study was conducted to determine the range of forces a bent-cap connection would be required to develop. Significant tension forces can develop in cap-to-column connection reinforcement as a result of longitudinal and transverse moments developed in the substructure. This indicated the need to investigate anchorage requirements for connection reinforcement between cast-in-place columns and precast cap.

There are also implementation issues that must be addressed to permit the use of precast substructure connections on construction sites. Erection of precast bent-caps will require tight tolerances. Most bridge contractors have little experience with precast bent-cap construction. Guidance needs to be provided to precast manufactures and bridge contractors to ensure the successful use of this product.

The main objective of the TxDOT-sponsored Project No. 1748, Development of a Precast Bent Cap System, is to develop a connection detail

which is both constructable and has the ability to transfer the necessary forces between a column or pile and precast bent-cap.

The research project has been divided into three phases. Each phase is explained briefly in the following sections.

1.2 OVERVIEW OF RESEARCH PROJECT

1.2.1 Phase I-Connection Design and Pullout Tests

Phase I, which was the lengthiest and most fundamental portion of Project 1748, required approximately 1.5 years to complete. At the start of the research project, the following work plan was used to guide the activities of the research team.

1. Survey existing literature
2. Identify products for anchorage and coupling
3. Study existing bridges with precast bent-caps
4. Develop candidate connection details
5. Test selected details in laboratory
6. Develop final details and design methodology
7. Prepare final report

The first four items and a portion of the fifth were completed in Phase I. The literature survey revealed that precast substructures have been used in a number of projects in recent years. However, most of the emphasis in the applications was on connections that used post-tensioning schemes to connect

precast elements. The Florida Department of Transportation (FDOT) contracted LoBouno, Armstrong and Associates (LAA), reported in Reference 1, to develop a family of standardized shapes and connection details for precast substructures. The connections developed by LAA required extremely small construction tolerances and incorporated proprietary connection hardware. In addition, no testing of connections was performed.

For the second item, available products for anchorage and coupling of reinforcing bars were identified. They include headed reinforcement, mechanical couplers, and grouted-sleeve couplers. Products selected for use in the research projects were chosen considering their effectiveness, availability, and relative costs.

The third task in the work plan was a study of existing bridges where precast bent-caps were used. TxDOT recently constructed two bridges with precast bent-caps: 1) Red Fish Bay and Morris & Cummings Cut Bridges on State Highway 361 (1995), reported in Reference 2, and 2) Pierce Street Elevated Freeway on Interstate Highway 45 (1997). The construction operations were carried out promptly in both projects, but there was room for improvement in the connection details, in relation to potential durability concerns related to shrinkage in the grout pocket.

Based on the survey of previous projects, available connection hardware, and review of related literature, various connection details were developed. They fall into four basic categories:

1. Grout Pocket Connections
2. Grouted Vertical-Duct Connections
3. Bolted Connections
4. Grouted Sleeve-Couplers

In development of candidate connection details, economics, constructability, durability, and force transfer issues were carefully considered. TxDOT personnel and a group of industry representatives contributed significantly to the development of details. A complete discussion of the candidate connection details can be found in Reference 1.

The last activity of Phase I was to evaluate the force-transfer characteristics of reinforcing bars anchored in grout pockets and grouted ducts. Eighteen single-line grout pockets, six double-line grout pockets, and eight grouted vertical-duct connections were tested in Ferguson Structural Engineering Laboratory. The pullout tests for the various connections provided important data related to development length, significance of grout strength, and confinement provided by pocket confinement steel and metal ducts that were used in the proportioning and detailing of Phase II test specimens. The complete discussion of Phase I tests is reported by Waggoner [2] and Matsumoto [4].

1.2.2 Phase II-Connection Tests

Phase II used the knowledge developed in Phase I to proportion an approximately full-scale bent-cap-to-pile connection and bent-cap-to-column

connections. The connections included grouted-pocket, grouted vertical-duct and bolted connections subjected to realistic loads. Not only was the force transfer investigated but also: 1) suitability of gravity-flow grouting, 2) practical limits for the bedding layer depth, 3) cracking at the bedding layer, and 4) overall behavior of the connections. The four specimens tested in Phase II included:

1. Single-Line Grout Pocket Connection
2. Double-Line Grout Pocket Connection
3. Vertical-Duct Connection
4. Bolted Connection.

Multiple hydraulic rams were used during testing to generate different loading conditions. Both service-level and factored-load tests were conducted on each specimen. In the following chapters, the construction sequence and test program for each specimen are described with results of each test.

1.2.3 Phase III-Large Scale Connection Tests

Phase III involved the construction of two full-scale bents incorporating vertical-duct, grout-pocket, and bolted connections. The test specimens were intended to determine constructability of different connection types with the help of a contractor. The two bents constructed were a precast trestle-pile bent with four 16 in. piles, and a precast cap on three 30 in. diameter cast-in-place columns. Both bents were 25 ft. long and had a 33 in. x 30 in. rectangular cross section. Phase III was still underway when this thesis was completed. The results from the Phase III tests will reported by Matsumoto [4].

1.3 OBJECTIVE

This thesis covers the work performed in Phase II of the TxDOT Project No. 1748 research program. Phase II was intended to test the adequacy of grout-pocket, vertical-duct, and bolted precast bent-cap-to-cast-in-place column/pile connections. Test specimens were proportioned based on preliminary design methods developed in Phase I. Results of the Phase II tests will be used to finalize design recommendations presented in the final project report.

CHAPTER 2

DESCIPTION OF PHASE II TEST PROGRAM

2.1 INTRODUCTION

The main objectives of the Phase II tests of the TxDOT Project 1748 research program were to evaluate constructability, determine the influence of the bedding layer on connection behavior, and assess the behavior of connection details under realistic loads. For this purpose four connection specimens with various details were designed and constructed. The connections tested included:

1. Single Line Grout Pocket Connection (P2-SLE)
2. Double Line Grout Pocket Connection (C2-DL)
3. Vertical Duct Connection (C2-VD)
4. Bolted Connection (C2-BC)

The results of Phase I tests, reported by Waggoner [1], provided a wealth of basic behavioral data. This information was used to proportion connections for the Phase II tests. A variety of the most promising connection types identified or developed in concert with the industry advisory panel, reported by Matsumoto [5], were selected for testing in Phase II. The variables for Phase II tests are shown in Table 2.1.

Table 2.1 Phase II Test Variables

Test	Connector	Grout	Shims
P2-SLE Pile-Single Line 1/3, Embedded Pile	3 #9 epoxy-coated bars; 15 in. Embedment; #3 @ 4 in. spiral confinement	Euclid Hi-Flow	Two 3 in. x 3 in. steel shims (Longitudinal Direction)
C2-DL CIP Column Double Line 2/2	4 #9 epoxy-coated bars; 15 in. Embedment; #3 @ 4 in. spiral confinement	Sika 212	Two 3 in. x 3 in. steel shims (Longitudinal Direction)
C2-VD CIP Column Vertical Duct 2/2	4 #9 epoxy-coated bars; 15 in. Embedment; 4 in. ducts; #3 @ 4 in. spiral confinement	Masterflow 928	Two 3 in. x 3 in. Polyethylene shims (Longitudinal Direction)
C2-BC CIP Column Vertical Duct 2/2	4 1 in. diameter threaded rods (B107); 3 in. ducts; #3 @ 4- in. spiral confinement	Masterflow 928	Two 3 in. x 3 in. Polyethylene shims (Longitudinal Direction)

2.2 SPECIMEN DESIGN AND CONSTRUCTION

Each specimen consisted of a precast bent-cap segment and a pile or column segment. The pile or column segment was cast with a footing that was anchored to the laboratory test floor.

For the first specimen, P2-SLE, a 16 in. square pile was embedded into the bent-cap. For the other specimens C2-DL, C2-VD, and C2-BC, a 30 in. diameter cast-in-place column was connected to the bent-cap segment.

Design loads consistent with the type of construction (precast pile vs. cast-in-place) were calculated accordingly. The maximum vertical load for the pile

case was 200 kips and was 550 kips for the column cases. Design moments were determined using longitudinal and transverse eccentricities of 7 in.

All bent-caps had a cross section that was 30 in. deep and 33 in. wide. The lengths of the caps were 12-ft. Reinforcement details for the precast caps were designed to preclude flexural, shear or torsion failure of the caps before strength of the connection was developed.

2.2.1 Single Line Grout Pocket Specimen (P2-SLE)

The P2-SLE precast cap segment had 4 #11's at top and bottom, and 2 #5's on side faces as longitudinal reinforcement. The top rebars were anchored using 90-degree hooks. Number 5 closed ties were placed approximately every 8 in. Reinforcement details for the P2-SLE specimen are shown in Figure 2.1.

The grout pocket was formed at the center of the precast cap segment. The block out for the single line connectors had an 8 in. x 12 in. cross-section at the bottom and tapered in both directions to 10 in. x 14 in. at the cap top. There was a base void of 20 in. x 20 in. in cross-section that was 3 in. deep. This base void provided a space for embedment of the pile top. To shape the pocket inside the cap during concrete casting, styrofoam was used. The styrofoam was precut to the pocket dimensions and was attached inside the formwork (see Figure 2.2). The pocket was confined with a #3 spiral with 4-in. pitch. After casting concrete, the styrofoam was dissolved with gasoline.

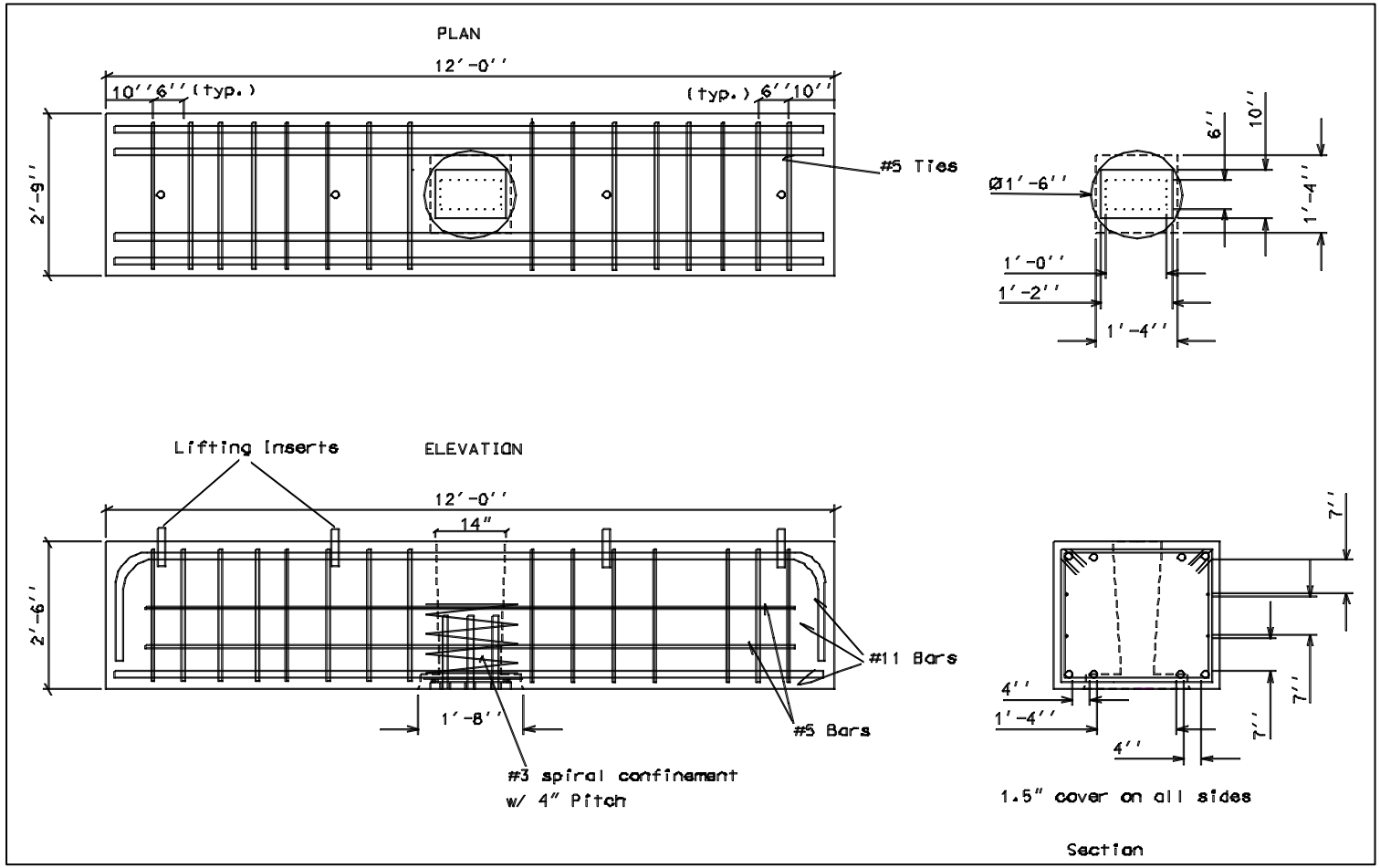

Figure 2.1 P2-SLE precast bent-cap segment reinforcement details

The pile segment used to support the precast cap segment had a 16 in. square cross section and 2 ft. height. The pile was cast together with an 18 in. deep, 68 in. square footing. The footing was used to tie the test specimen securely to the strong floor of the laboratory. Figure 2.3 shows the reinforcement cage for the pile and footing combination.

Figure 2.2 Styrofoam block out inside the formwork

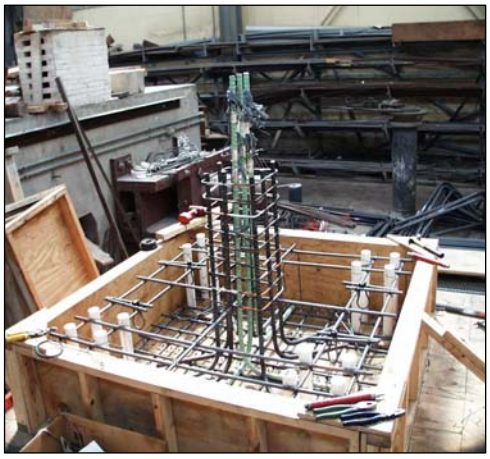

Figure 2.3 Pile and footing reinforcement

The pile had 8 #8 longitudinal reinforcing bars. Bars had a 90-degree hook on one end and were anchored inside the footing. Number 3 closed ties were placed at every 4 in. along the pile height.

For connecting the pile to the P2-SLE precast cap, 3 #9 epoxy-coated bars were used. These bars were inserted in the core of the pile segment, and were anchored in the footing with 90-degree hooks. Based on the results of the Phase I tests, Waggoner [3], a 15 in. embedment length for the epoxy-coated bars was provided at the top of the pile. These epoxy-coated rebars were placed at a 3.5 in.

spacing on the centerline of the transverse direction of the pile.

The footing was cast first, then the top of the form was closed, and finally the pile was cast. Concrete was cured for three days and then the formwork was removed.

2.2.2 Double Line Grout Pocket Specimen (C2-DL)

The C2-DL precast cap segment reinforcement details are shown in Figure 2.4. It had 10 #11's at the top, all of which were anchored using 90-degree hooks at both ends. Additionally, there were 4 #11's at the bottom and 2 #5's on each side face for longitudinal reinforcement. Two #6 closed ties were bundled together and placed every 6 in. along the cap.

Styrofoam was again used to shape the block outs inside the cap. Block outs had a 3 in. x 16 in. cross section at the bottom and were tapered slightly in both directions to 5 in. x 18 in. at the cap top. Unlike the P2-SLE cap, there was no base void for the column embedment. The pockets were confined with a #3 spiral with 4-in. pitch. The styrofoam was later dissolved with gasoline after casting concrete. Figure 2.5 shows the reinforcement cage inside the formwork.

The column segment for supporting the cap had a 30 in. circular cross section and was 2 ft. high. It was cast together with a footing similar to that described for the P2-SLE specimen. The column had 8 #9 longitudinal bars that were anchored inside the footing. The longitudinal rebars were confined with a 24 in. diameter spiral with 6-in. pitch. Figure 2.6 shows the reinforcement cage for the column-and-footing segment.

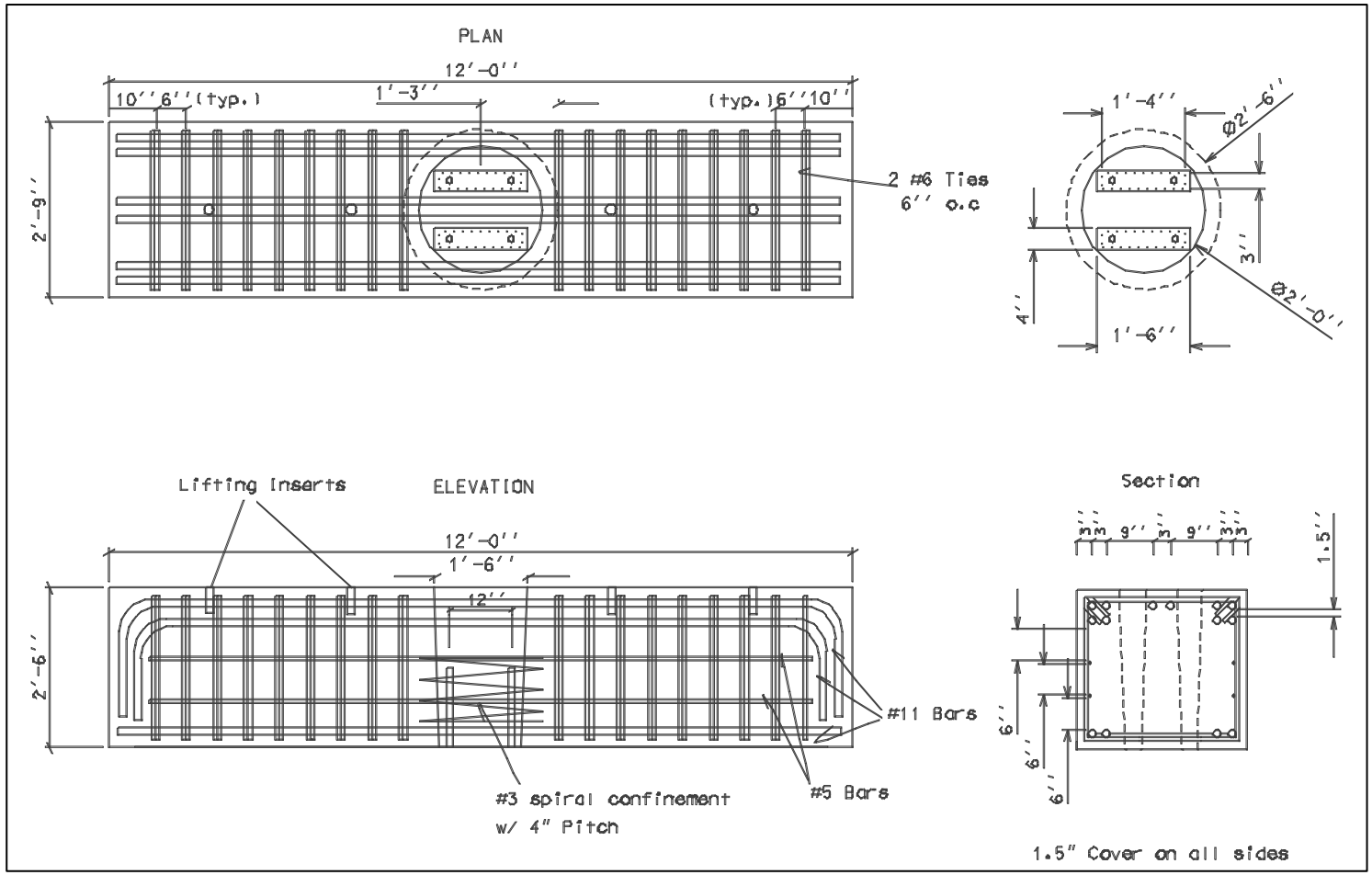

Figure 2.4 C2-DL precast bent-cap reinforcement details

Four #9 epoxy-coated rebars were used to connect the column to the cap beam. These were also hooked at one end and anchored inside the footing. The straight bar anchorage length inside the bent-cap was 15 in.

Figure 2.5 Reinforcement cage for C2-DL cap

Figure 2.6 Reinforcement cage for C2-DL column and footing

2.2.3 Vertical Duct Specimen (C2-VL)

Figure 2.7 shows the reinforcement and the duct details for the C2-VD precast cap. The cap beam had reinforcement details identical to those used in the C2-DL precast beam. The difference between the two specimens was the connection type. Galvanized, deformed metal ducts were placed in the cap instead of formed grout pockets.

Four 4 in. diameter metal ducts with 30 in. height were placed inside the cap before casting. The ducts were tied to adjacent rebars to maintain their position during casting. A 24 in. diameter spiral with 4 in. pitch confined the ducts. Figure 2.8 shows the reinforcement cage and ducts before casting.

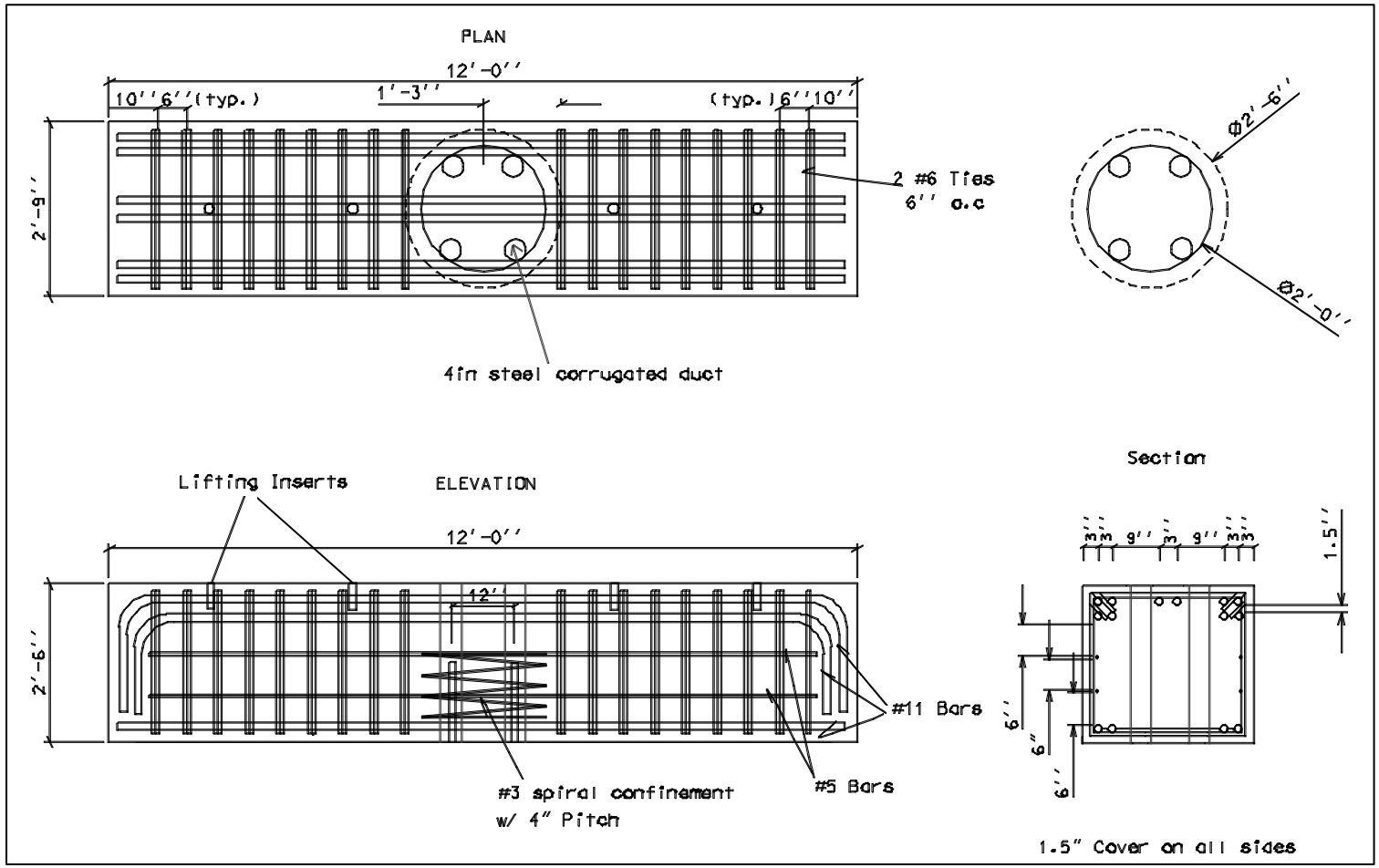

Figure 2.7 C2-VD precast bent-cap reinforcement details

The column-and-footing segment was reinforced similar to the column-and-footing segment used in specimen C2-DL. Four #9 epoxy-coated rebars were located in the core of the column and were anchored with hooks in the footing. These bars were used to connect the bent-cap segment and the column. A 15 in. embedment length in the cap for the epoxy-coated bars was provided.

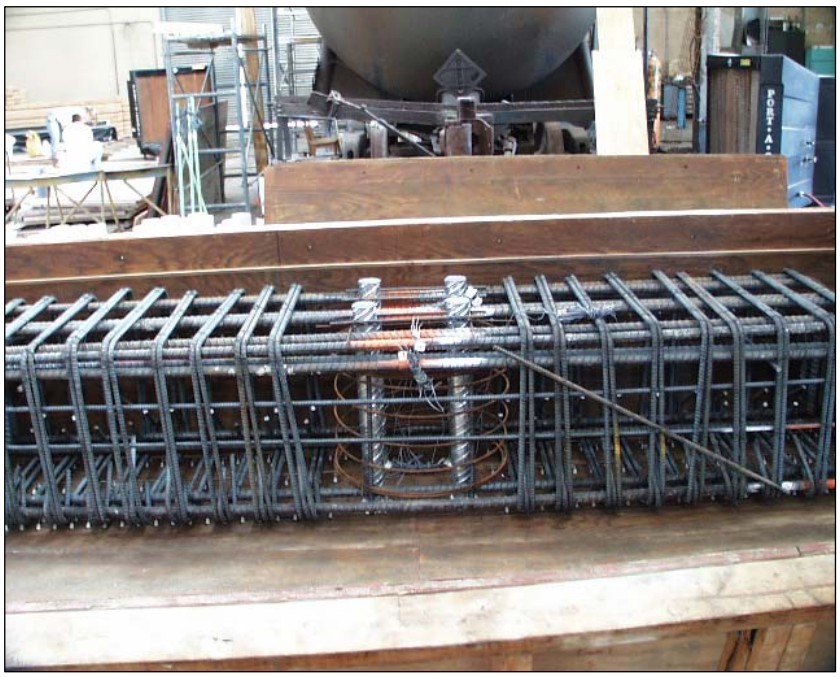

Figure 2.8 Reinforcement cage for C2-VD cap

2.2.4 Bolted Connection Specimen (C2-BC)

The precast bent-cap reinforcement details for specimen C2-BC (Figure 2.9) were the same as for specimens C2-DL and C2-VD. For this specimen, 3 in. diameter galvanized, deformed metal ducts were used in the connection region.

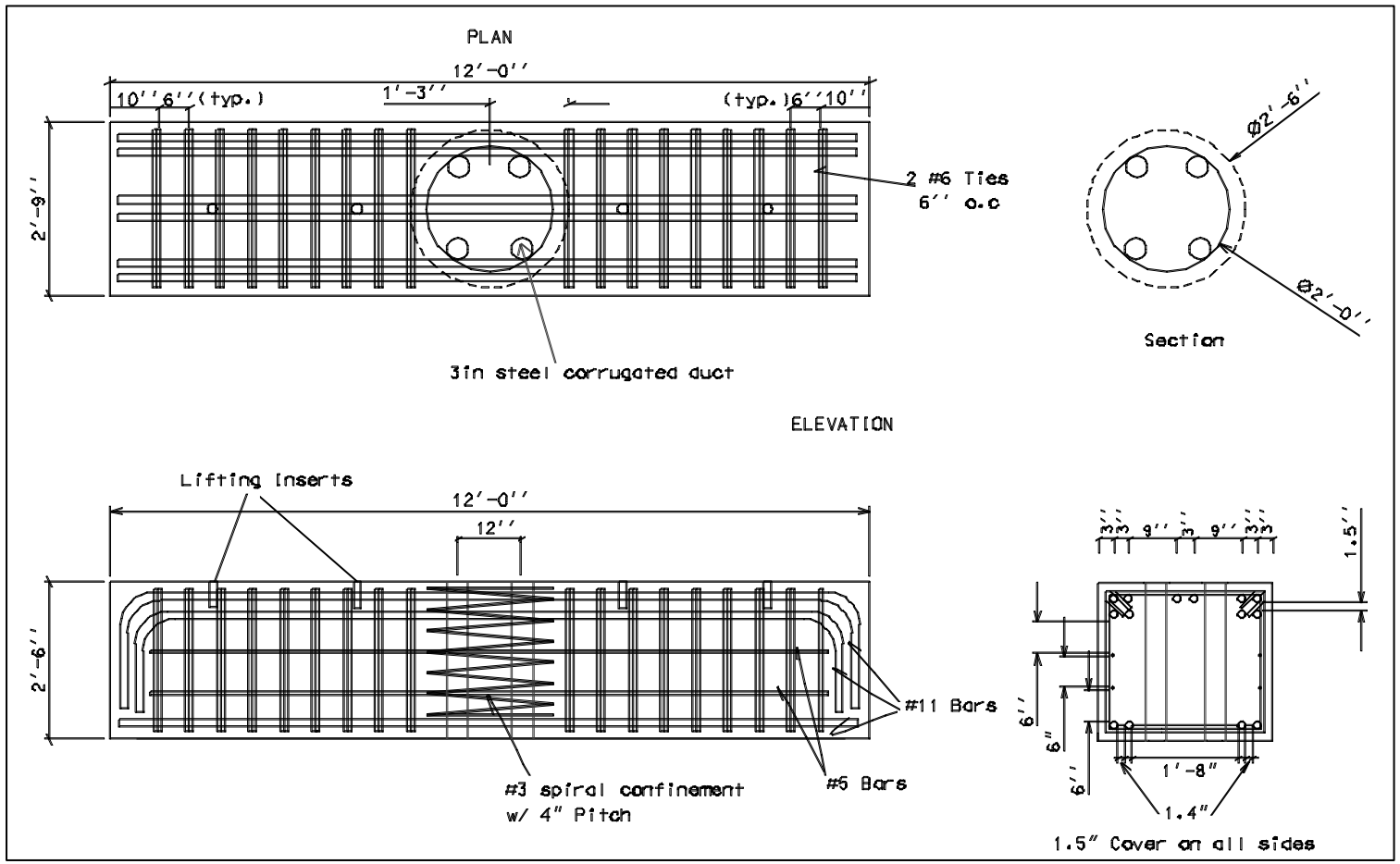

Figure 2.9 C2-BC precast bent-cap reinforcement detail

The confinement spiral extended to the top of the beam and had smaller pitch near the top of the cap to resist bearing stresses from the bolted connection.

The column-and-footing assembly for the C2-BC specimen was constructed after testing the C2-VD specimen. During C2-VD tests, some cracking was observed in the footing. This led to an increase in the size of reinforcement used in the footing for the C2-BC specimen. Number 6 rebars were used instead of #5's.

For connecting the cap to the column, four 1 in. diameter threaded rods were placed inside the column core. The bars were anchored inside the footing by attached plates. The bars were cut sufficiently long to ensure they would pass through the metal ducts inside the cap and still have the necessary length to accommodate bolts at the top. Figure 2.10 shows column-and-footing assembly before casting.

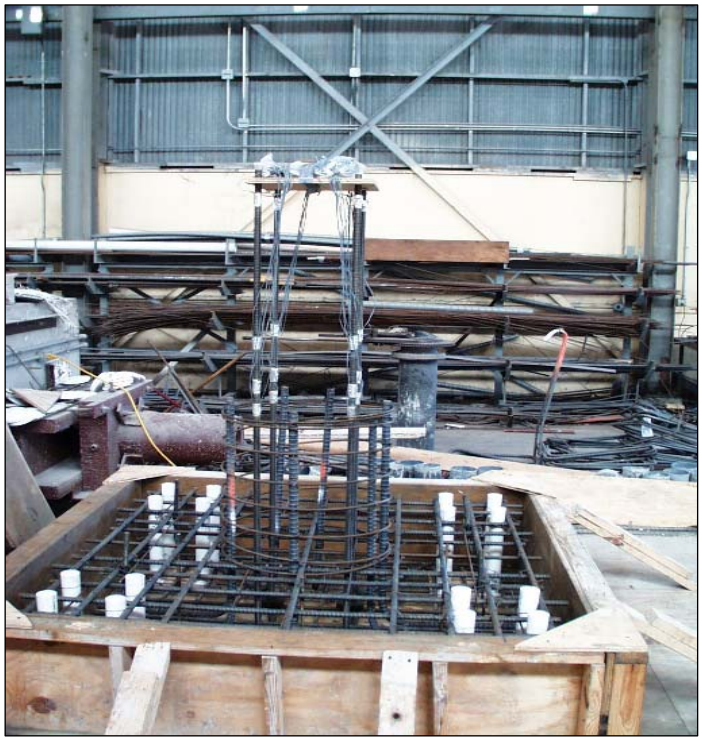

Figure 2.10 Reinforcement cage for C2-BC column and footing

2.3 GROUTING OF SPECIMENS

Grouting of the pockets and ducts was performed through a series of steps. The pile or column surface was first prepared, then the cap was placed over this surface. Next, the opening between the pile or column and cap was closed with formwork, and grout vents were installed. Finally, the grout was mixed and placed. The following sections describe the details of the grouting operation for each specimen.

2.3.1 Grouting of Single Line Grout Pocket Specimen

Cap placement and pre-grout set-up: The footing and 16 in. pile with a single line arrangement of the three epoxy-coated #9 connectors are shown in Figure 2.11. All Phase II specimens, except the bolted connection, had 15 in. embedment of the epoxy-coated bars into the cap. Two 3 in. x 3 in. x 1.5 in. steel shim stacks were used in setting the P2-SLE cap. The strain gage lead wires attached to strain gages on the bars are also visible in the photograph.

Figure 2.11 Shims and connectors

After the cap was placed on the shims, three wooden posts were used to provide additional stability until the grout was placed. Figure 2.12 shows the cap in its final position. The block out for accepting the single-line connectors is shown in Figure 2.13 from the cap top. The strain gage lead wires were taped neatly on the cap top prior to the grouting procedure.

Figure 2.12 Cap in final position

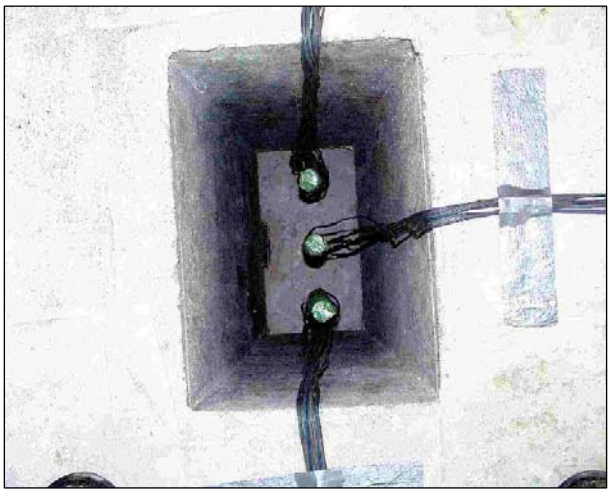

Figure 2.13 Single line block out with bars

Grouting: After setting the cap and bedding form, four 0.25 in. inside diameter vent tubes were placed through holes drilled in the bedding form, which were near the corners (see Figure 2.14). Prior to grouting, pocket surfaces were pre-soaked to limit absorption of grout water into the cap and to verify sealing of the bedding form. Excess water that did not flow out the vent tubes was vacuumed out of the pocket.

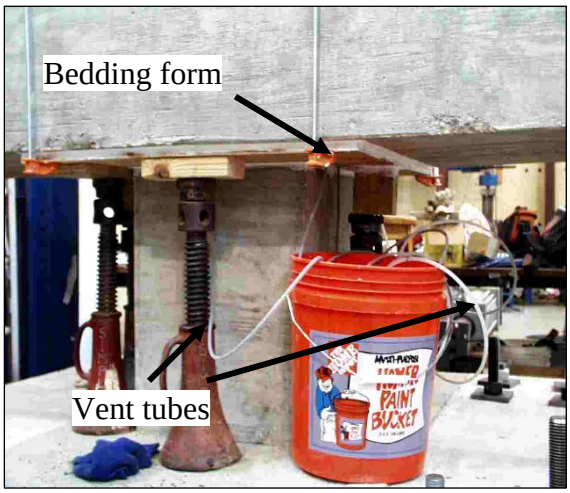

Figure 2.14 Bedding form and vent tubes

Euclid Hi-flow was used for grouting specimen P2-SLE to check the impact of a lower-strength grout on connection performance. Ten 55 lb. bags were mixed in a paddle-type mortar mixer with 11.5 lb. of tap water per bag, which was within the manufacturer's recommended range. The mixing was performed at 75º F and 70% humidity. During mixing, the grout appeared stiff, which led to the addition of an extra half gallon of water per bag. After mixing for five minutes (manufacturer recommended 4 minutes), a flow cone test was

performed on the grout, per CRD-C611. The test produced a 57-second flow which was slightly high (20-30 seconds is desirable). There was also some clumping of material during mixing as shown in Figure 2.15. Mesh opening was 0.5 in. x 0.5 in.

Figure 2.15 Clumps observed during grouting

Grout was transported from the mixer to the specimen using 5-gallon buckets. It was poured against a wall of the pocket to limit the introduction of air inside the pocket. After tamping the first lift of grout, which filled approximately 5 in. of the pocket depth, the vent tubes were opened to allow grout to flow out and to help remove any entrapped air at the bedding layer. Grouting was completed in six lifts with each layer tamped with a rod.

After completing the grouting operation, the top surface of the grout was covered with a curing compound. The curing compound was applied for three days and then the bedding form was removed.

2.3.2 Grouting of Double Line Grout Pocket Specimen

Cap placement and pre-grout set-up: The footing and 30 in. circular column with the double line arrangement of four epoxy-coated #9 connectors are shown in Figure 2.16. The figure also shows a small cardboard ring, 0.25 in. thick, used to form the bedding layer. Four vent tubes with 0.5 in. inside diameter provided the means to vent air during grouting. Strain gauge lead wires are also evident.

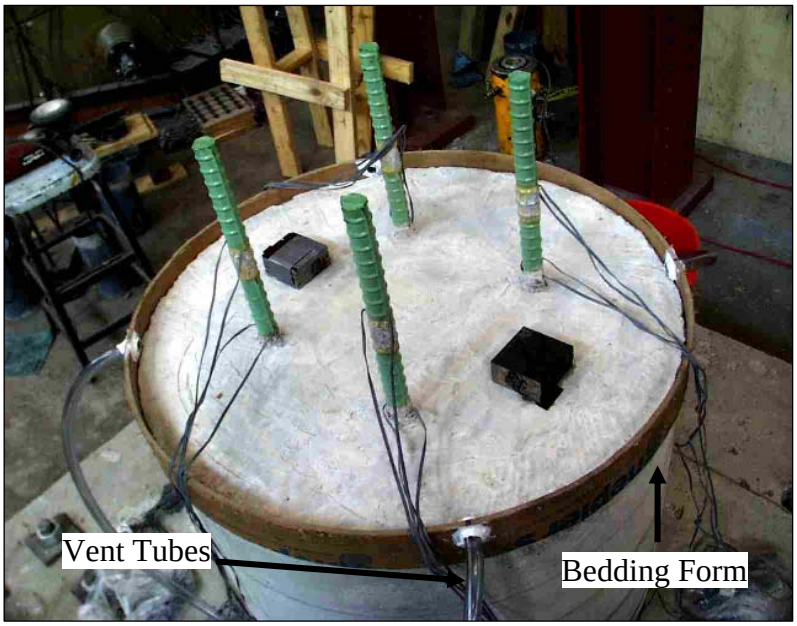

Figure 2.16 Column preparation for grouting

Two 3 in. x 3 in. x 1.5 in. steel shim stacks were used for supporting the cap prior to and during grouting. A few thin steel strips were used together with the shims to level the cap in the transverse and longitudinal directions. Shims

were glued to the surface with epoxy to prevent movement during cap placement.

Figure 2.17 shows the block outs for the double line connectors. The block outs (dimensions provided in Section 2.2.2) provided sufficient tolerance during placement of the cap. These V-shape block outs differed from the P2-SLE specimen's block out, which included a base void for embedment of the pile into the cap. The cap-to-column connections had bedding layers that were exposed. A 15 in. bar embedment was provided as the length of bar contained within the block out.

Grouting: After setting the cap, edges of the bedding form were caulked to prevent leakage during grouting. Prior to grouting, pocket surfaces were moistened.

Sika 212 was used for grouting. Unlike Euclid High Flow, Sika 212 was expected to produce desired grout strengths. In previous uses, Sika 212 was observed to have a relatively short working time (approximately 15 minutes). It was used in specimen C2-DL to investigate the impact of placement difficulties on connection performance. Seven 55 lb. bags were mixed with 10 lb. of water per bag. The mixing was performed in the shade at a temperature of 81^{o} F and 74% humidity. After mixing 5 minutes, a flow cone test was performed. A 17-second flow was obtained, which was in the desired range. During mixing, the grout appeared very fluid. However, following mixing, considerable segregation of sand and paste was evident.

Grout was poured against a piece of plywood to limit the introduction of air into the pockets (as shown in Figure 2.18). Grout was placed in the pockets in

several lifts, and was tamped with a rod. Due to segregation, dense aggregate accumulated at the bottom of the pockets, while the more fluid portion of the grout rose to the top. After tamping the first lift, the caulked ends of the vent tubes were opened to allow grout to flow to help remove any entrapped air in the bedding layer.

After grouting was completed, a several inch layer of water appeared at the top surface of the pockets. Because of this, curing compound was not sprayed on the pocket top. The day after grouting, most of the fluid had evaporated, leaving approximately a 2 in. void at the top of the pockets. Voids like this may pose durability concerns in the field if not topped off later with grout.

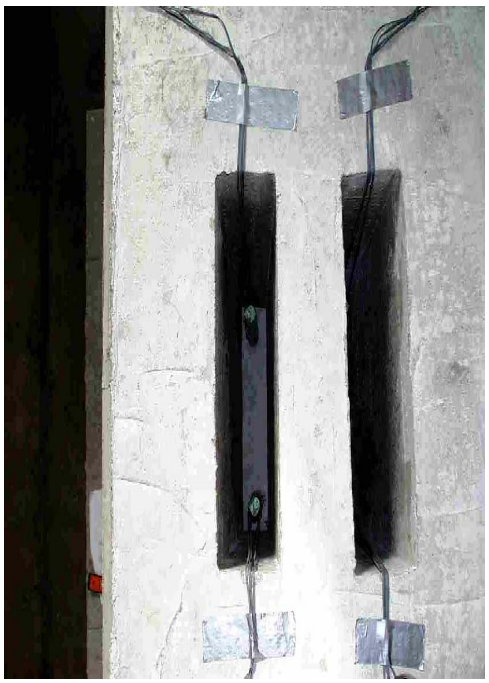

Figure 2.17 Block outs

Figure 2.18 Placement of grout

2.3.3 Grouting of Vertical Duct Specimen

The footing and 30 in. column with four epoxy-coated #9 connectors for specimen C2-VD were quite similar to those for specimen C2-DL (Figure 2.16). Two 2.5 in. x 5 in. x 1.5 in. polyethylene shim stacks were used rather than steel shims. The same preliminary grouting steps, described for specimen C2-DL, were used for specimen C2-VD.

Masterflow 928 grout was used for this specimen. Based on earlier tests, this grout was believed to provide the best overall performance. Six 55-lb. bags were mixed with 10 lb. of water. Grouting was performed at a temperature of 81º F and 78% humidity. During mixing, mortar appeared to be very flowable and uniform without any visible segregation. The flow cone test produced a 34-second flow.

Grout was poured in a duct through a funnel with a 1 in. inside diameter hose as shown in Figure 2.19. The end of the hose was placed very close to the bedding layer and the funnel was kept full while continuously placing grout to limit the air introduced inside the duct and bedding layer. Four 5 gallon buckets of grout were used to fill the bedding layer and four ducts. The grout surface at the top of the cap was covered with curing compound for two days. After three days, the bedding layer form and vent tubes were removed. Grout on the outer surface of the bedding layer appeared to be quite competent.

Figure 2.19 Funnel and hose used for grouting

2.3.4 Grouting of Bolted Connection Specimen

Grouting of the bolted-connection specimen was very similar to grouting of the vertical-duct specimen. After moistening the ducts, six 55 lb. bags of Masterflow 928 were mixed with 10 lb. of water per bag. The temperature was 95º F and the humidity was 40% during mixing. Due to high temperature, the flow cone test produced a 53-second flow.

The same funnel and hose used for placing grout in the C2-VD connection were used for this connection. A continuous flow of grout through the funnel filled the bedding layer and ducts. Care was taken not to get grout on the protruding portions of the threaded rods. Figure 2.20 shows the end of the grouting procedure.

The top surface was sprayed with a curing compound for three days. After three days of curing, nuts were installed on the threaded rods and were tightened with a torque wrench to 200 lb-ft.

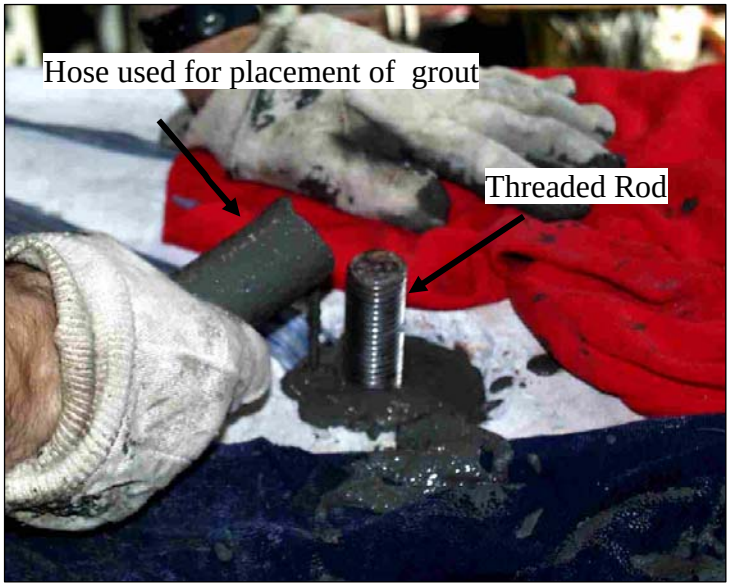

Figure 2.20 Threaded rod and grout

2.4 MATERIALS

2.4.1 Steel

Reinforcing steel used for preparing the specimens was Grade 60 and was supplied by a local company. The #5 longitudinal rebars, hooked #11 bars, and #5 and #6 closed stirrups were manufactured prior to delivery to the laboratory.

The #9 epoxy-coated rebars used to connect the bent-caps and columns or piles were Grade 60. They were supplied by Fletcher Coatings Company. Epoxy coating was done in accordance with ASTM A775.

For the C2-BC specimen, 1 in. diameter B107 threaded rods were used.

Table 2.2 lists the yield and ultimate strength of the #9 epoxy-coated rebars and 1 in. threaded rods.

Table 2.2 Connector Bar Strengths (ksi)

	Lab Test	
Connector	Yield	Ultimate
#9 Epoxy-coated	66	110
1 in. Threaded rod	89	111

2.4.2 Concrete

The ready-mix concrete was delivered by Capitol Aggregates Company. A TxDOT Class C mix with a required 28 day compressive strength of 3600 psi was used for all specimens. A slump of 4 in. was ordered but on-site slumps varied.

Table 2.3 shows the mix used. Concrete casting was conducted on five separate occasions. The P2-SLE and C2-DL bent-caps were cast during the first casting operation. The C2-VD cap and P2-SLE footing were cast during the second operation. The C2-BC cap and C2-DL footing were the third casting, and the C2-VD footing and C2-BC footing were the fourth and fifth castings, respectively.

The concrete compressive strength for the separate castings was monitored with 6 in. x 12 in. cylinders at 3, 7, 14, 28 and 56 days. An additional three cylinders were also tested on the day connection test was initiated. Figure 2.20 shows the strength histories for the five different castings.

Table 2.3 Concrete Mix

Cement lb/yd³	¾ in Coarse Aggregate lb/yd³	Fine Aggregate lb/yd³	Water lb/yd³	Retarder oz/yd³
564	1882	1191	225	24

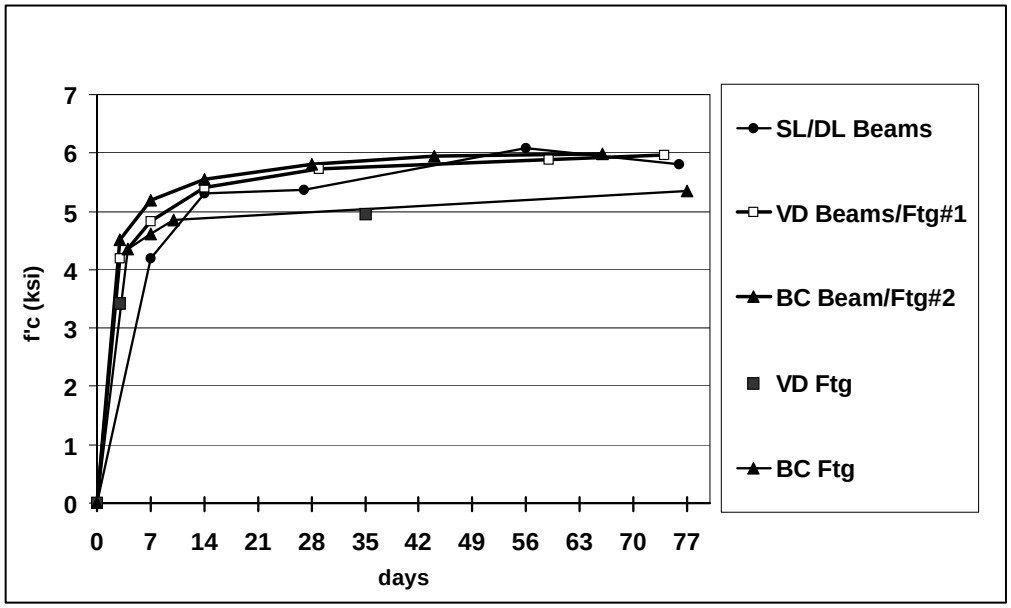

Figure 2.21 Concrete compressive strength histories

2.4.3 Grout

Three different grouts were used in the testing program. These included:

1. Euclid High Flow by Euclid Corporation
2. Sika 212 by Sika Corporation
3. Masterflow 928 by Masterbuilders Corporation

The prepackaged grouts come in 55-pound bags. The amount of water mixed with each type of grout varied by manufacturer.

Standard 2 in. grout cubes were tested at 1, 3, 7 and 28 days in accordance with ASTM C109 and C1107. The strength of the grout cubes is presented in Figure 2.22.

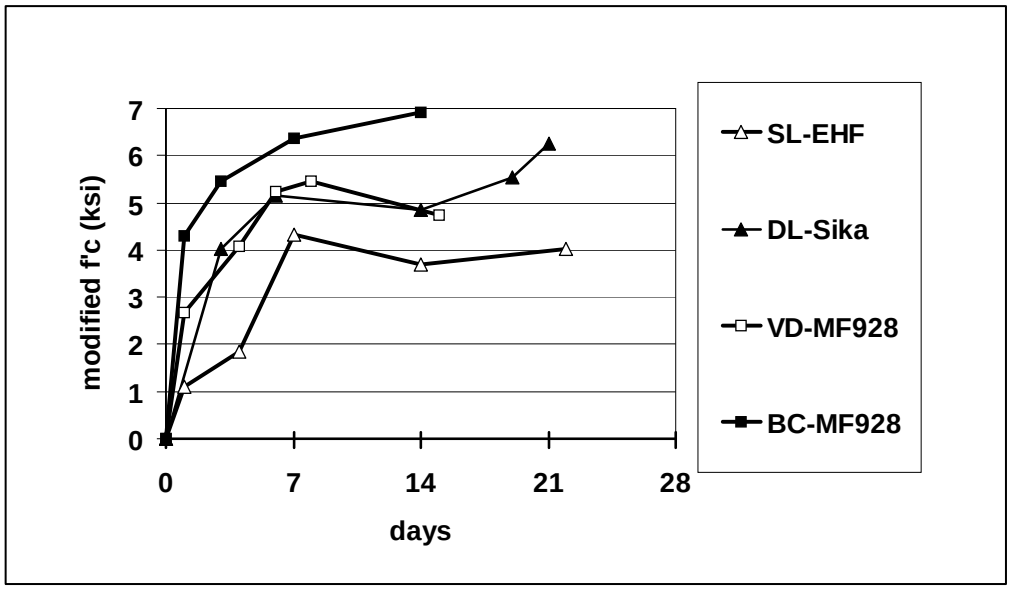

Figure 2.22 Grout strength histories

2.5 INSTRUMENTATION AND MEASUREMENT

During testing, deflection, strain, and load measurements were taken. For deflection measurements, spring-loaded linear potentiometers were used. Figure 2.23 shows a schematic of linear potentiometer locations on the specimen. The potentiometers on the bent-cap measured the transverse and longitudinal displacements of the cap during loading. Additional transducers were placed on the grout surfaces to measure the grout/concrete and grout/duct slip. The linear

potentiometers on the footings were precautionary to measure any slip or uplift of the footing during loading. However, measurements taken showed that displacement of the footings was effectively negligible.

Strain measurements were made on the connection bars, threaded rods, and vertical ducts. Connection bars were first ground smooth on the surface at the specified locations to provide a surface to apply the strain gages. Then the surfaces were cleaned with diluted acid and base, and strain gages were attached on these surfaces. The stain gauges were located on opposite sides of the bar at 1, 7.5 and 14 in. from the top of the bedding layer.

Threads on the threaded rods were also ground off at specified locations and the smooth surface was cleaned with diluted acid and base. Strain gages were located on opposite sides of the bar at –1, 1, 15 and 29 in. from the top of the bedding layer.

Vertical ducts used in specimens C2-VD and C2-BC were also gauged to monitor the circumferential strains in the duct. Gauges were located at 1, 7.5 and 15 in. from the bottom of the ducts. For the ducts in the C2-VD specimen extra gauges were placed parallel to the deformation on the duct at 1 and 7.5 in. in order to monitor deformations along the seams.

Load measurements were taken with load cells and pressure transducers. For the vertical loads applied on the cap, pressure transducers were used to monitor pressure in hydraulic cylinders used to apply the load. During testing of specimen P2-SLE two rams were used on top of the cap. Both of these two rams were connected to pressure transducers. In other tests, four rams were used and

only two of them, the southeast and northwest rams, were connected to the pressure transducers. The ram, which applied transverse load to the cap, was monitored with a load cell.

All deflection, strain and load measurements were monitored electronically and recorded using a data acquisition system. In addition to these measurements, cracks were marked and measured with a crack-width comparator.

2.6 TEST SET-UP

The testing apparatus used to load the bent-cap connections is shown in Figure 2.24. The loading frame consisted of four columns, two long girders and two cross beams. The rams on the bent-cap reacted against the crossbeams that were bolted to girders, which transferred load to the columns. Girders and crossbeams were both W30x108 sections. Columns were bolted to the strong floor, which has a capacity of 200 kips/column.

A longitudinal eccentricity at the connection was produced when the rams were offset from the bent-cap centerline, this produced. To test for different transverse eccentricities, the west crossbeam was moved further from the connection.

The transverse ram supported by wooden pedestals at the east end of the cap was loaded occasionally during testing to observe transient loading effects, such as wind and braking, on the behavior of the connection.

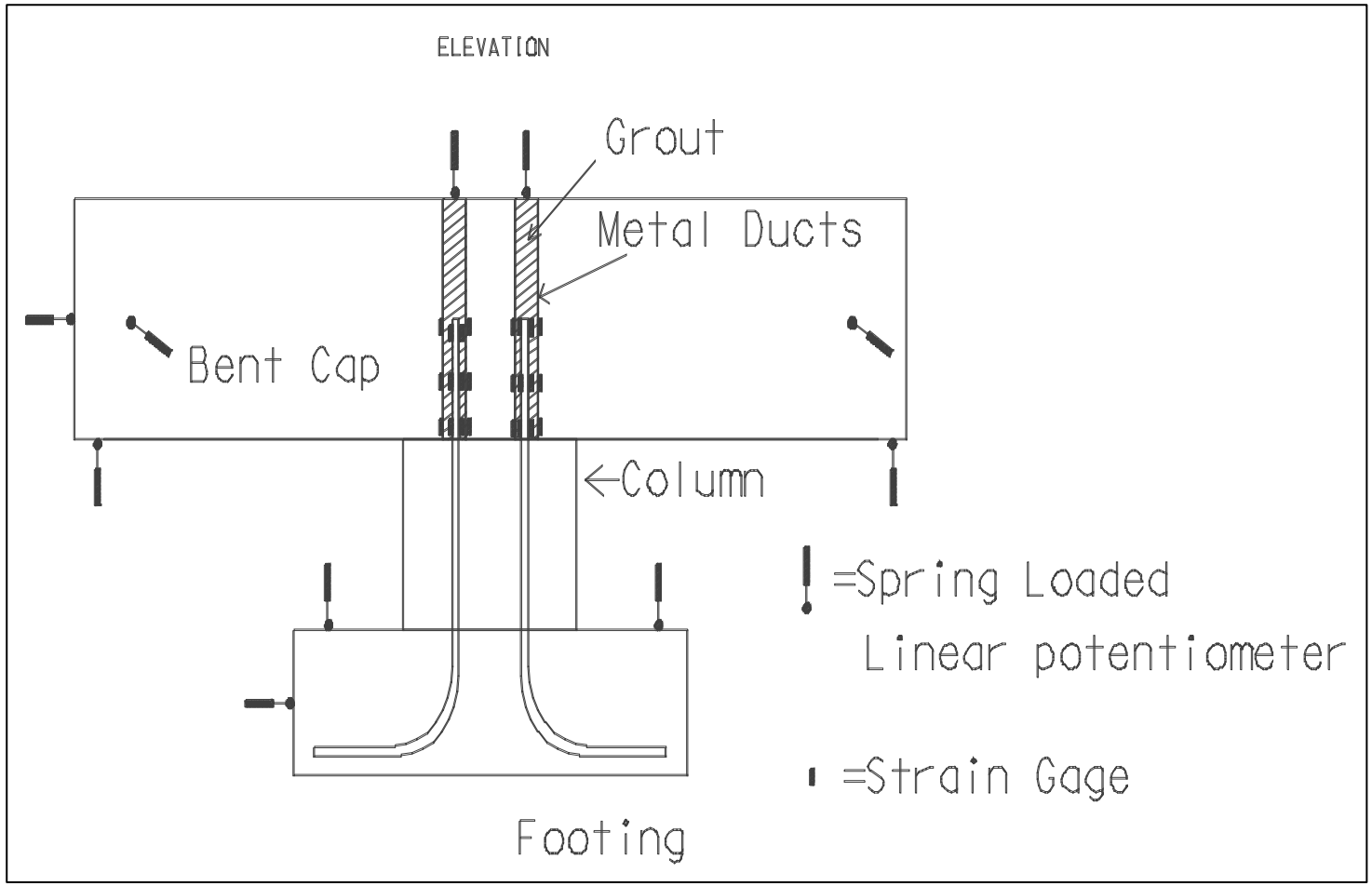

Figure 2.23 Instrumentation schematic

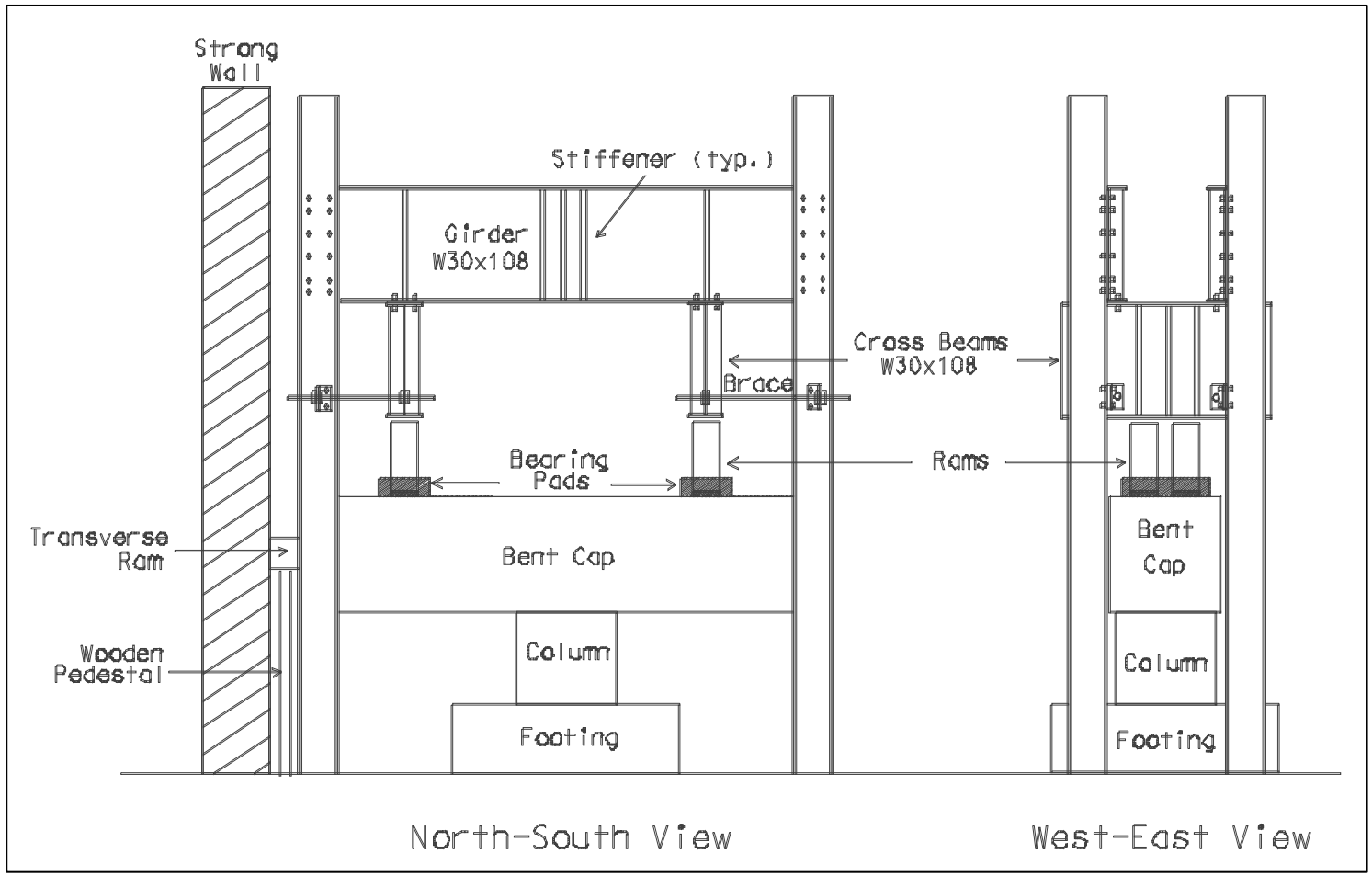

Figure 2.24 Typical test setup

CHAPTER 3

RESULTS OF SINGLE-LINE GROUT POCKET TESTS

3.1 INTRODUCTION

The single line grout pocket tests investigated the adequacy of a cap-and-pile connection. A single line of three epoxy-coated #9 bars with 15 in. embedment depth and low-strength grout were used in the connection. Additionally, working time for the grout and quality of the grout near the top surface were investigated because of concerns raised during Phase I tests.

Six tests incorporating different eccentricities and loading conditions were conducted on the specimen. The load sequence shown in Table 3.1 was used to subject the connection to increasingly severe load combinations.

Two vertical rams were used to apply vertical load and transverse and/or longitudinal moments to the connection, while a horizontal ram was used to apply shear on the connection. Based on typical conditions for trestle-pile bents, a maximum factored load of 100 kips on each side of the connection (total load, including dead load) was selected, together with eccentricities in the 3 to 7 in. range. These loads and eccentricities were considered proof loads for the connection. Larger eccentricities and loads were used to precipitate a connection failure after proof loads were applied.

Table 3.1 Loading History

P2-SLE Test No.	Eccentricity, e (in)		Applied Load (kips)		Notes
	Trans.	Long.	Vertical	Horizontal	
1	3.75	0	94	0	Low e_trv; first cracking
2	3.75	3	92	0	Combined eccentricities
3	6.75	0	92	0	Higher e_trv
4a	6.75	3	66	21	Application of shear
4b	6.75	3	94	21	Application of shear
5a	6.75	6	65	20	Failure eccentricities
5b	6.75	6	92	20	Failure eccentricities
6a	6.75	9	65	20	Failure eccentricities
6b	6.75	9	95	20	Failure eccentricities
6c	6.75	9	105	19	Failure eccentricities

3.2 TEST RESULTS AND GENERAL BEHAVIOR

3.2.1 Test 1

Before Test 1 was initiated, pre-existing cracks in the grout pocket and specimen were examined. Figure 3.1 shows the top surface of the single line grout pocket. The surface had a pumice stone-like appearance, which made measurement of existing cracks and identifying the new cracks difficult. Air bubbles that rose to the top of the grout formed large craters directly above the epoxy-coated bars. The very permeable appearance of the exposed grout surface raised concerns about the durability of the Euclid High Flow grout. In addition,

hairline cracks, which formed due to dead load moments and construction loads, were observed on both side faces of the cap beam.

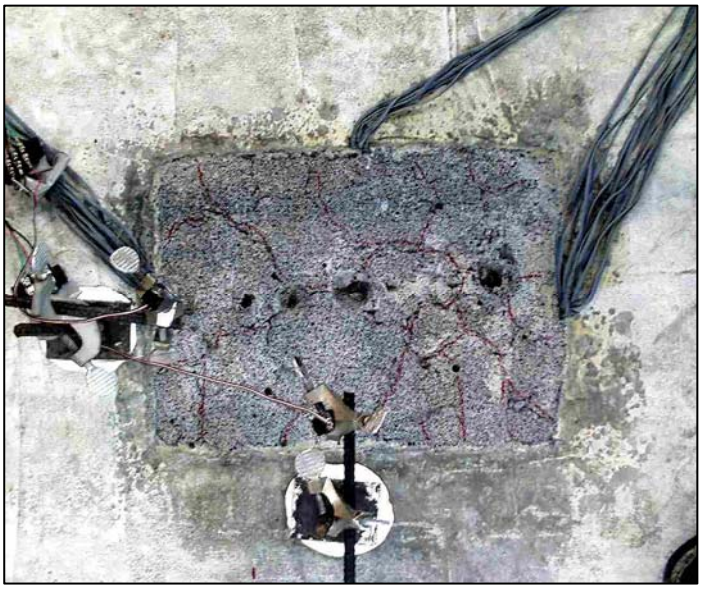

Figure 3.1 Condition of grout prior to testing

As the test started, new cracks appeared on the top surface of the cap at 61 kips applied on both ends of the cap. They extended from the pocket toward the edges of the cap beam. At 70 kips each end, corresponding to service level load, two new cracks formed at the pocket and other cracks extended down about half the depth of the beam. These cracks were a maximum of 0.005 in. wide. It was observed that the paths of flexural cracks joined the pre-existing grout pocket cracks, causing the grout pocket cracks to open. As mentioned earlier, cracks at the coarse surface of the grout pocket were difficult to identify and measure. It was apparent that some crack widths exceeded 0.10 in., while most were less than 0.007 in. This cracking and the larger surface voids mentioned earlier suggest

that paths for moisture ingress into the cap might exist.

Figure 3.2 shows a view of the specimen from the north side at the maximum factored load of 94 kips applied on both the west and east side. This was approximately 37% of the flexural capacity. As the load increased to maximum level, existing cracks extended and new cracks appeared across the width of the cap beam on both sides of the pocket. Figure 3.3 shows the top of the cap. The lack of reinforcement across the entire width of the beam, due to the presence of the single line pocket, enabled some cracks to open more in the center of the cap, but all flexural crack widths were well within 0.013 in.

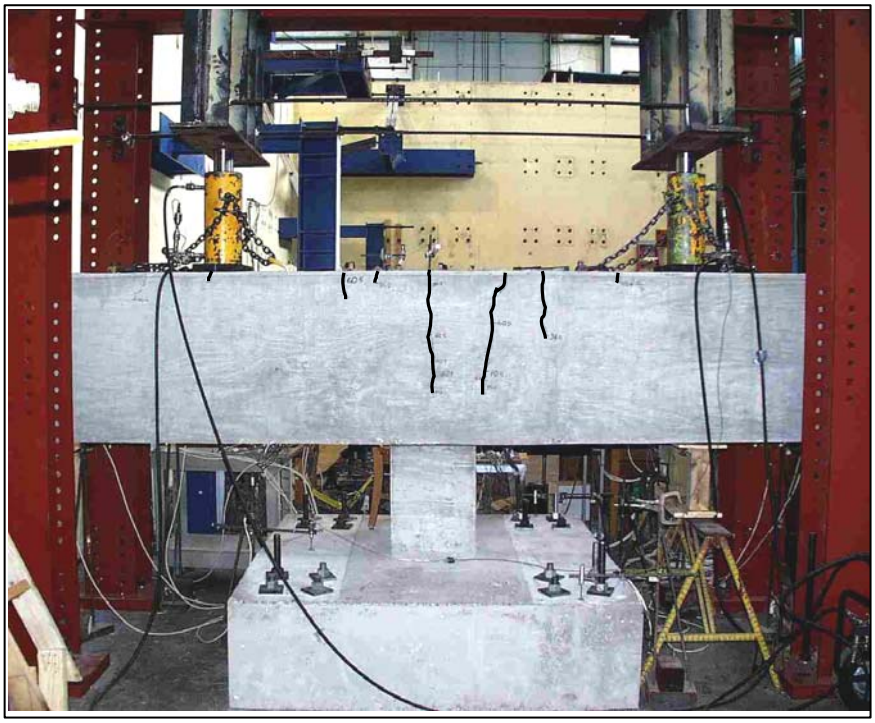

Figure 3.2 North side of specimen P2-SLE after Test 1

Figure 3.3 Top of the cap for specimen P2-SLE after Test 1

Figures 3.4 and 3.5 show the load-strain and load-displacement plots for Test 1, respectively. During the test, all connectors were in compression and sustained very low levels of stress. The maximum strain, measured 1 in. above the bedding layer on the west bar was less than 10% of nominal yield. The plots confirmed that stress dissipates along the length of the bars. Strains at 7.5 in. above the bedding layer were less than those at 1 in. above the bedding layer. The load-displacement response indicated some softening of the system as flexural cracking developed, especially beyond 61 kips. The maximum measured displacement was 0.12 in. at the west tip of the cap beam. Since there was no longitudinal eccentricity, the potentiometer readings on the same end of the cap

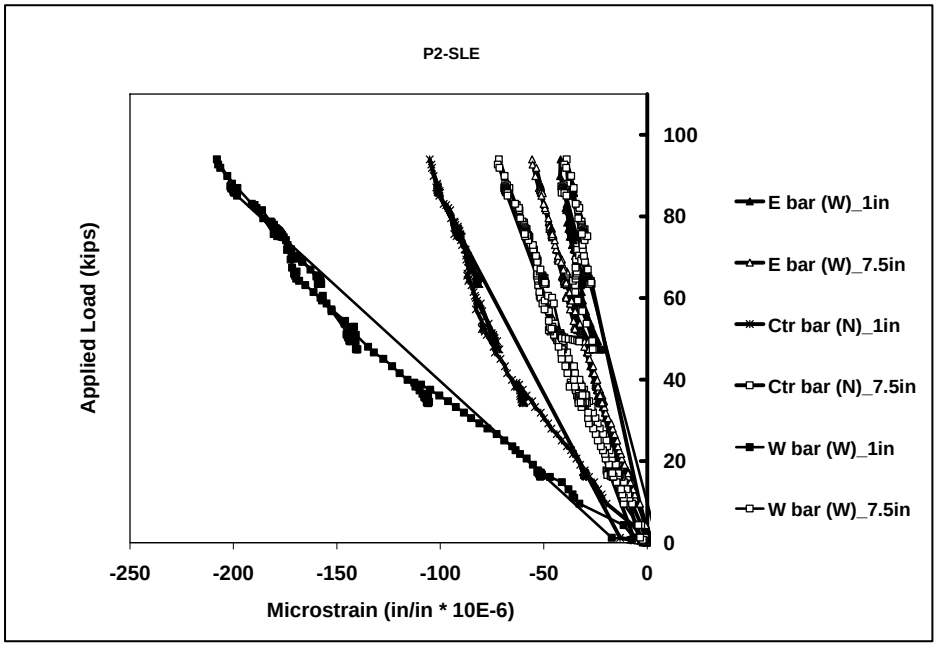

Figure 3.4 Load-strain response for Test 1

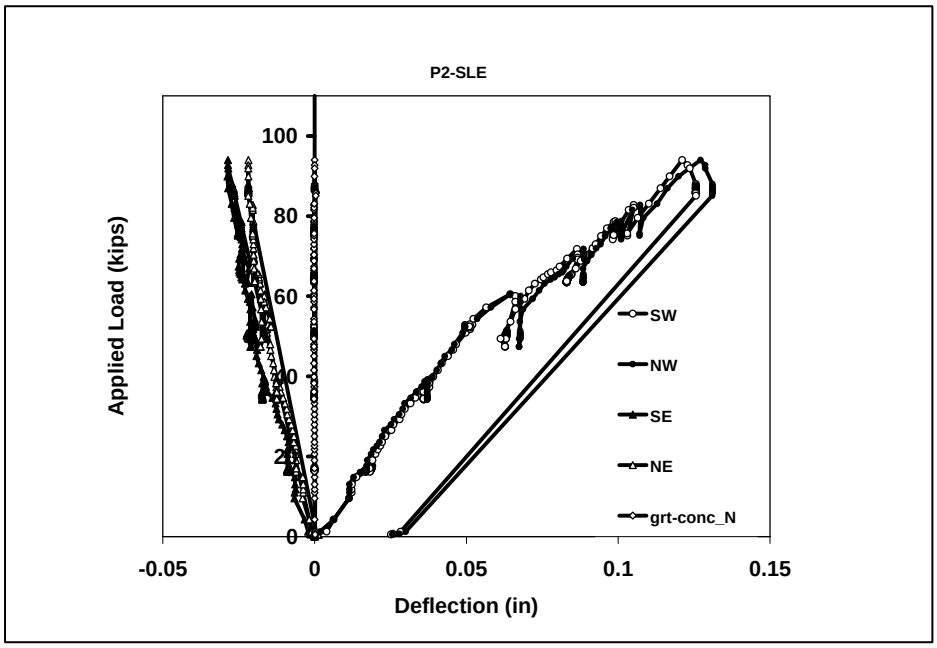

Figure 3.5 Load-displacement response for Test 1

beam were the same. Grout-concrete relative displacements were nearly negligible as shown in the displacement response.

3.2.2 Test 2

For Test 2, longitudinal eccentricity of the applied loads was increased to 3 in. to test the effects of combined transverse and longitudinal eccentricities. During the test a maximum load of 92 kips was applied to each side of the cap beam. Very little difference in behavior was observed compared to Test 1. The cracks reopened to slightly larger widths than in Test 1 and extended no more than approximately 3 in.

The load-strain and load-displacement plots are shown in Figures 3.6 and 3.7, respectively. Strain values at 1 in. above the bedding layer were similar to Test 1 results which were less than 10% of nominal yield. However, a reduction in compressive strains was observed in the center and east bars. Load-displacement response for the cracked cap was essentially linear, reaching a maximum tip deflection of approximately 0.14 in. Unlike Test 1, potentiometers on the same ends of the cap measured different displacements due to the longitudinal eccentricity. Grout-concrete relative displacements were negligible.

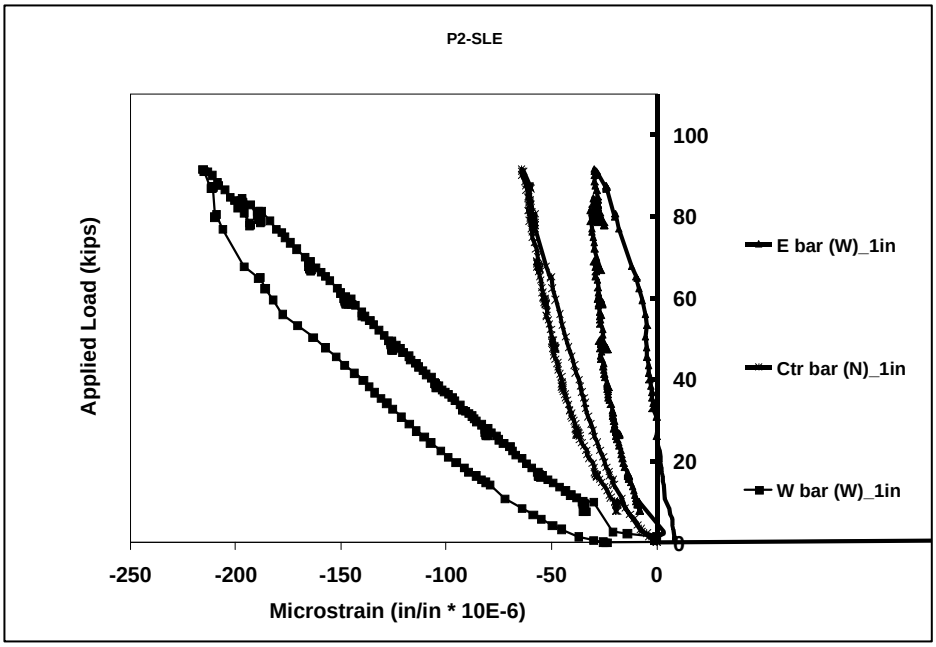

Figure 3.6 Load-strain response for Test 2

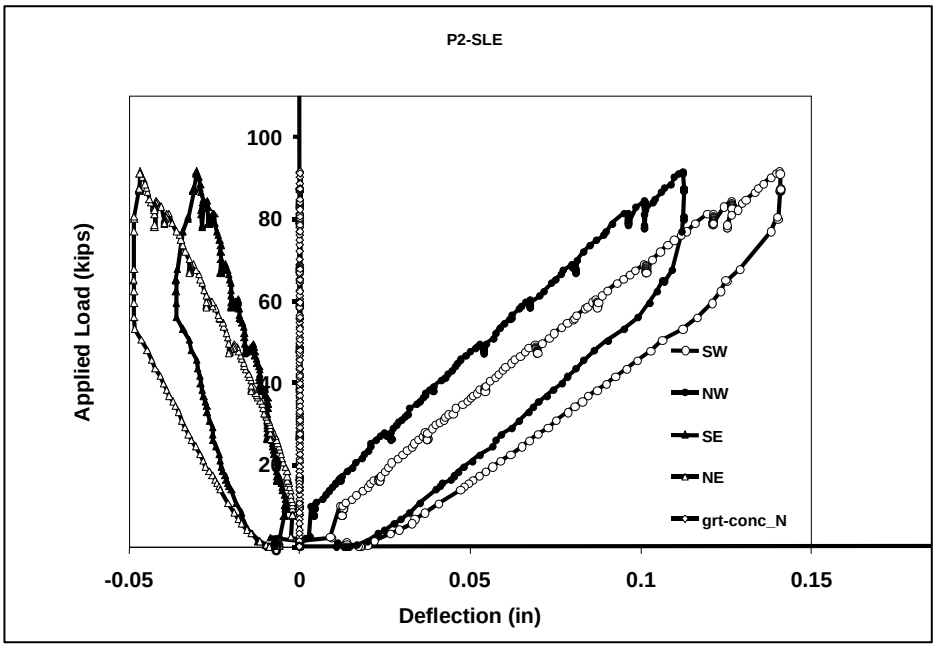

Figure 3.7 Load-displacement response for Test 2

3.2.3 Test 3

At a transverse eccentricity of 6.75 in., which was about twice that of earlier tests, new cracks appeared. A maximum load of 92 kips was applied to each end of the cap beam. The pre-existing cracks extended and opened to no larger than 0.013 in. At 62 kips, existing cracks extended slightly on the grout pocket surface. Near maximum load, popping sounds were audible and existing cracks extended further. Additionally, two cracks appeared on the tension (east) side of the pile. As illustrated in Figure 3.8, cracks wrapped around the entire east side and a few inches of the north side of the pile.

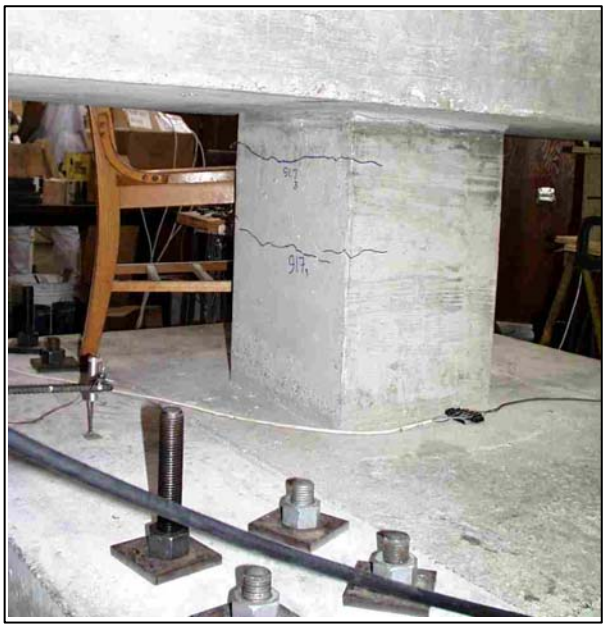

Figure 3.8 Cracks in the pile of specimen P2-SLE, Test 3

Strain measurements (Figure 3.9) indicated that tensile strains were developed in the east bar during testing. At about twice the transverse eccentricity of Test 1, the compressive strain in the west bar at 1 in. above the bedding layer increased to 15% of yield. Load-displacement response (Figure 3.10) for the cracked cap was essentially linear, with the west tip deflection reaching 0.22 in. Grout-concrete relative displacements were again negligible.

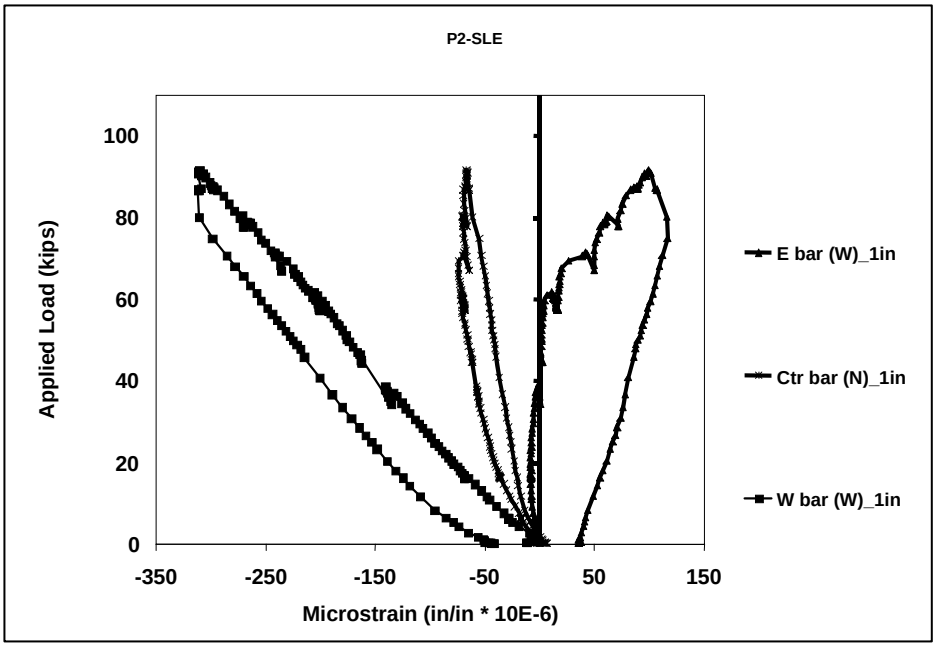

Figure 3.9 Load-strain response for Test 3

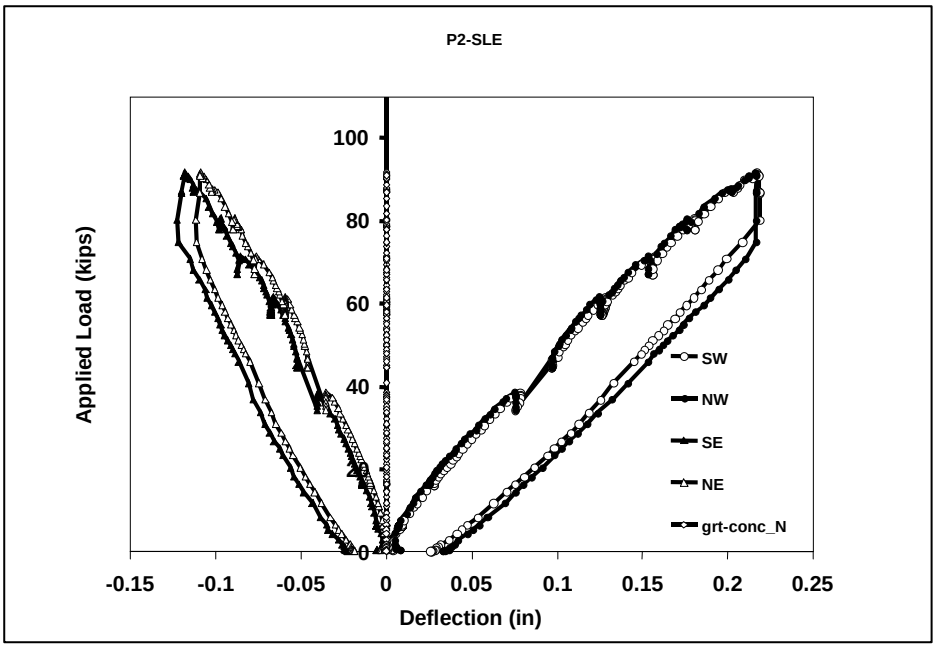

Figure 3.10 Load-displacement response for Test 3

3.2.4 Test 4

In addition to increased longitudinal eccentricity, a horizontal load of 21 kips along the longitudinal axis of the cap was applied at service and factored load levels. As loads were increased to the service level, cracks in the beam reopened and new cracks appeared in the pile. At 65 kips of vertical load applied to each end, the horizontal load was applied. This caused additional bending of the pile segment. Connection strains increased due to transverse loading. Increases were was most evident in the east bar. The strain at 1 in. above the bedding layer increased by 75% as shown in the load-strain response (Figure 3.11), although the maximum strain levels were still minor (approximately 15% of nominal yield). Horizontal and vertical cap deflections increased by approximately 50% to 0.08 in. and 0.24 in., respectively as shown in the load-displacement response (Figure 3.12). No change in the grout pocket surface cracking was observed.

After the lateral load was removed, vertical loads were increased to the factored load level of 94 kips, and the lateral load was then reapplied. An increase in response similar to Test 4a was observed. Tension was developed in both the east and center bars during loading. Pile cracks extended slightly and the maximum crack width at the northeast corner increased to 0.01 in. near the pile top. Grout-concrete relative displacements were negligible.

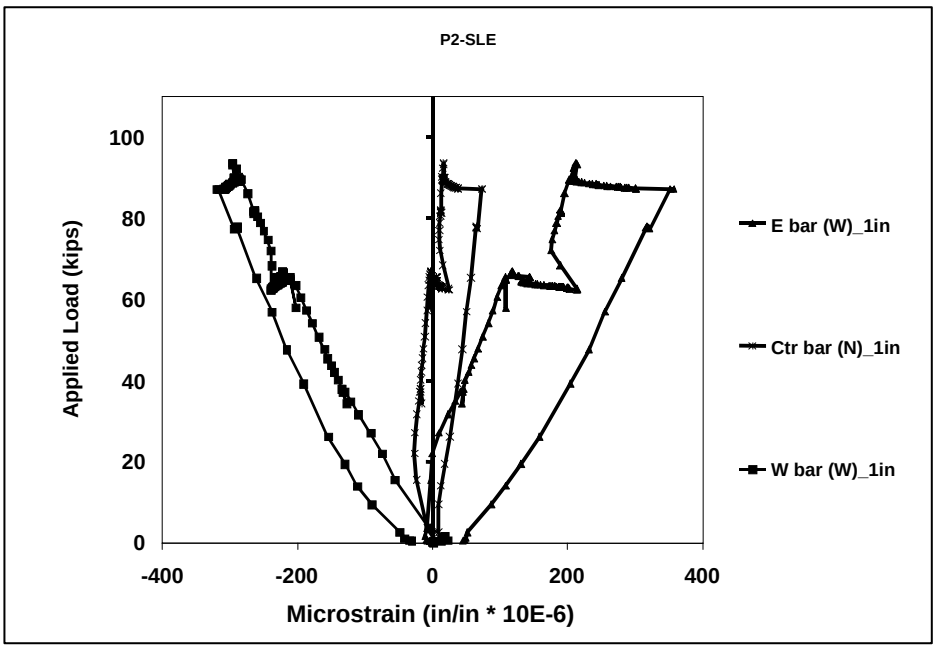

Figure 3.11 Load-strain response for Test 4

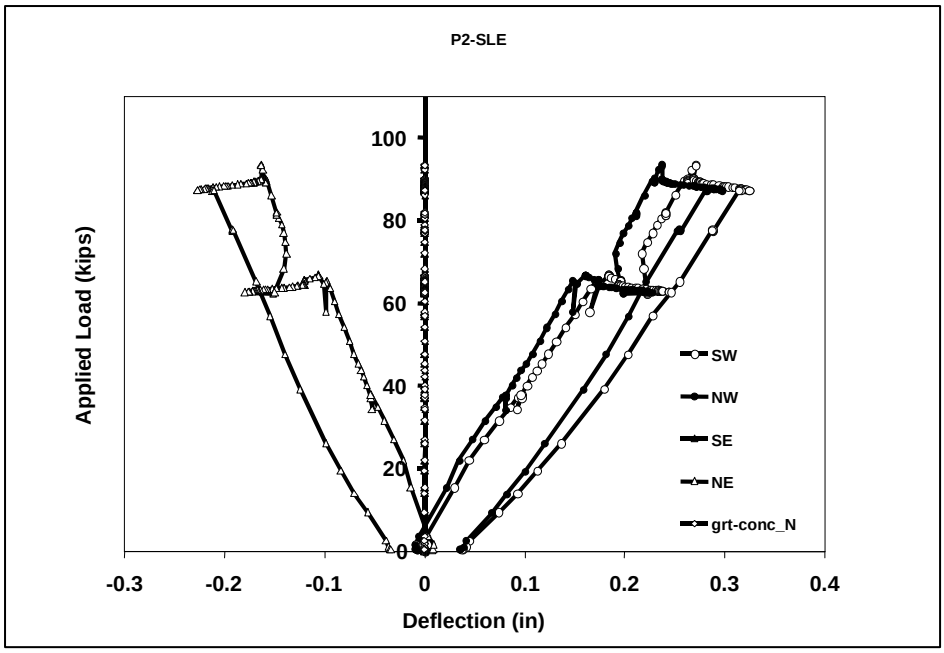

Figure 3.12 Load-deflection response for Test 4

3.2.5 Test 5

With an increased longitudinal eccentricity of 6 in., the connection was first tested at a service level of 65 kips applied to each end. Cracks on the north side of the pile extended as the load increased to service level. Figure 3.13 shows the cracks on the north side of the pile. The crack at the top opened to 0.09 in. at the northeast corner. The east and center connectors were strained in tension, with the largest measured strain being approximately 25% of nominal yield. The west connector was close to the neutral axis and was nearly unstrained throughout. Grout pocket cracks did not appear to open further, and grout-concrete relative displacements were negligible.

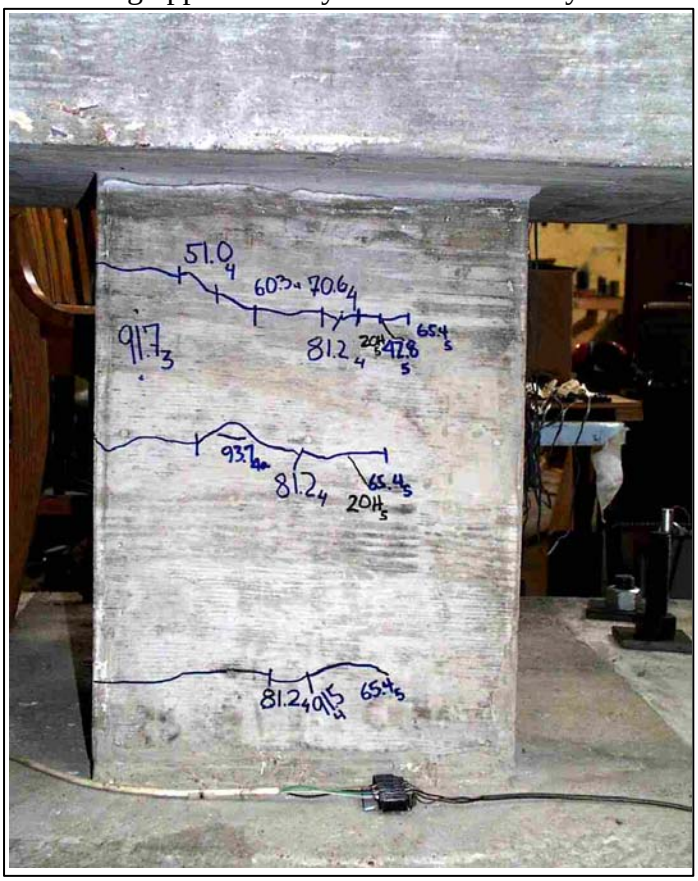

Figure 3.13 Cracks in the pile during Test 5

After removing the lateral load, vertical loads were increased to the factored level of 92 kips, then the lateral load was reapplied. Plots of strain and displacement, Figures 3.14 and 3.15, respectively, portray softer response at this load stage, which corresponds with the extension and formation of new cracks. Strain in the east bar at 1 in. above the bedding layer was approximately 50% of nominal yield. The east connector likely yielded several inches below the bedding layer. While this cannot be verified by strain measurements since gages were not located more than an inch below the pile top, residual vertical displacements after unloading suggest this. Vertical displacements were more than 0.40 in., and the cap beam side face deflected out of plane approximately 0.1 in., compared to 0.04 in. for Test 4b. Despite the large bar strains, grout pocket cracks at the surface did not appear to open beyond unloaded crack widths, and grout-concrete relative displacements were again negligible.

At 87 kips, a new crack near the pile top/bedding layer appeared on the tension side. This crack wrapped around the north and east faces of the pile and opened to 0.02 in. Other crack widths were 0.09 in. or less.

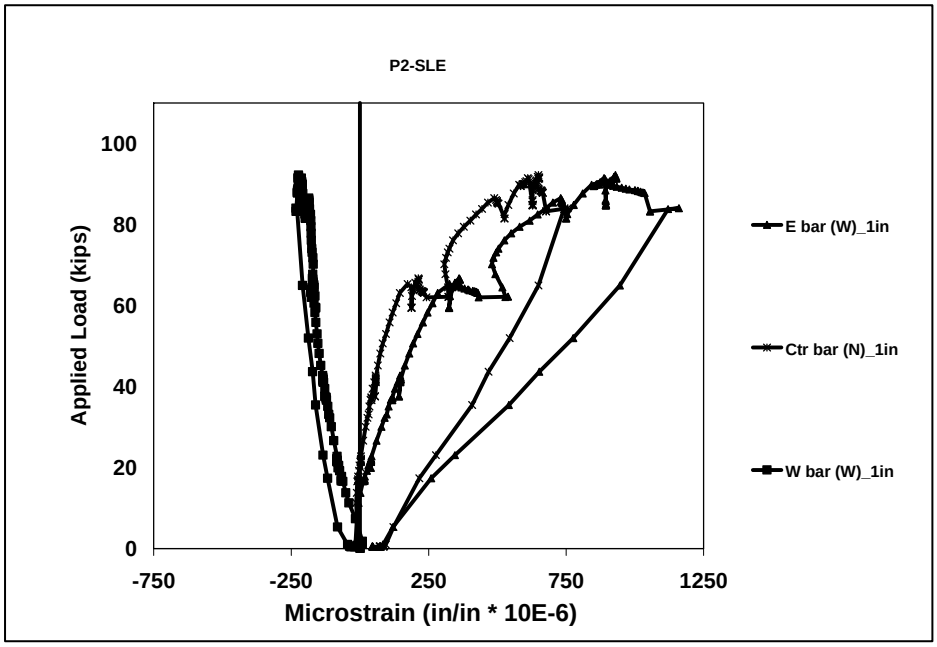

Figure 3.14 Load-strain response for Test 5

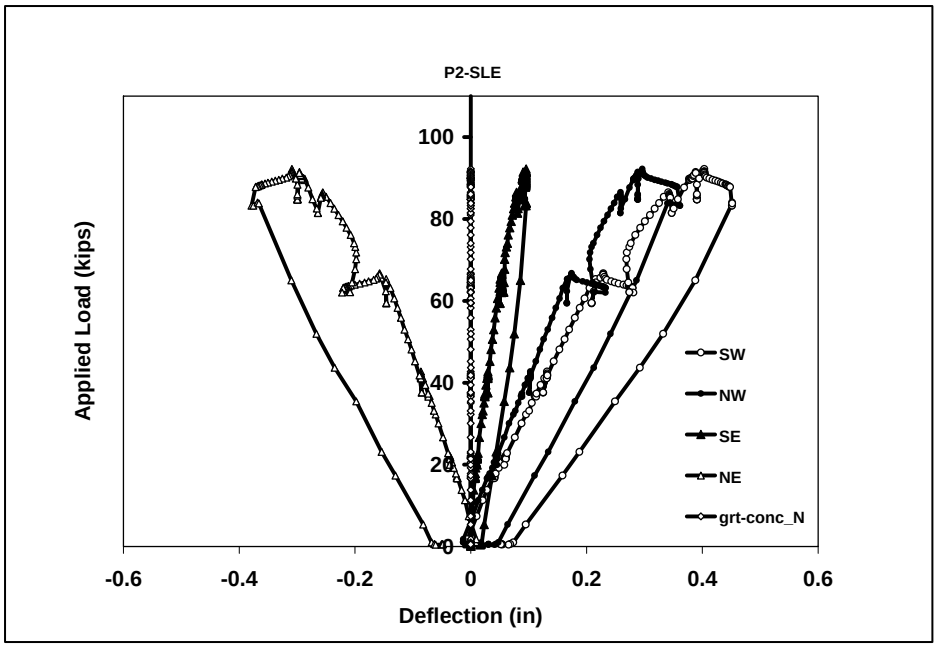

Figure 3.15 Load-deflection response for Test 5

3.2.6 Test 6

To initiate yielding of connectors, the longitudinal eccentricity was increased to 9 in. The strain and displacement responses for Test 6 are shown in Figures 3.16 and 3.17, respectively. At 65 kips, strain measurements indicated all bars to be in tension, with the east bar strain about 65% of nominal yield. The vertical cap displacement was approximately 0.4 in., and the lateral displacement was nearly 0.1 in. With application of the lateral load, the pile cracks opened significantly to 0.05 in. on the north and east faces. In addition, cracks appeared at the bedding layer on all sides of the pile.

After removing the lateral load, vertical loads were increased to the factored level of 95 kips, then the lateral load was reapplied. Similar to Test 5b, plots of strain and displacement portray softening of the system at this stage, corresponding to extension and opening of existing cracks and formation of new cracks. Multiple cracks at the bedding layer were observed. In addition, a large crack extended on the south side of the beam. This response indicated that one or more connectors yielded within the pile. This was confirmed by large residual vertical displacements.

Strain records showed the east bar reached yield strain on three sides of the bar, yet without overall bar yielding. Strain measurements indicated bending of the bar within the pocket such that strain on the south side of the bar was lower than yield, thus preventing overall yield of the bar. After applying the horizontal load, vertical displacements increased significantly to approximately 0.60 in., and the cap beam side face deflected out of plane to 0.24 in. Once again, grout pocket

cracks at the surface did not appear to open, and grout-concrete relative displacements were negligible.

In Test 6c, the connectors yielded. Even though yield of one or more of the connectors in the pile defined failure of the system, it was decided to further load the specimen in an attempt to yield the connectors within the grout pocket. In this way, the adequacy of the embedment depth and confinement under the most severe conditions could be investigated.

As illustrated by the load–strain diagram, at a slightly larger load of just 99 kips plus a horizontal load of 19 kips, strain records confirmed the east bar yielded one inch above and one inch below the bedding layer. As expected, this was accompanied by a large increase in system displacements. As the ram was further extended, the east bar began to strain harden, and at 105 kips the specimen was unloaded. Even at this state of loading, no change in the grout pocket surface cracking was observed, and no additional cracks formed around the pocket.

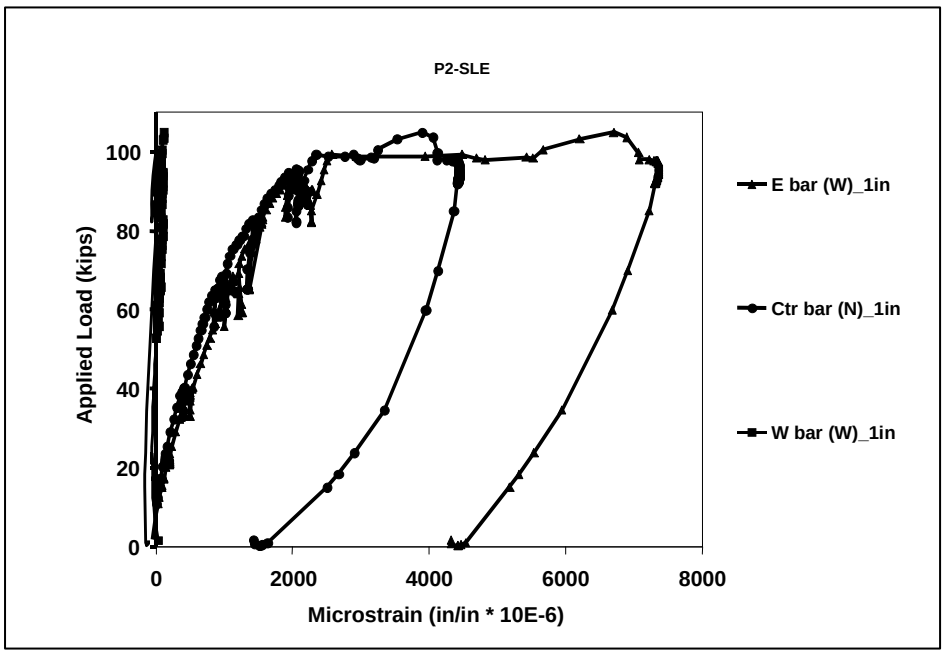

Figure 3.16 Load-strain response for Test 6

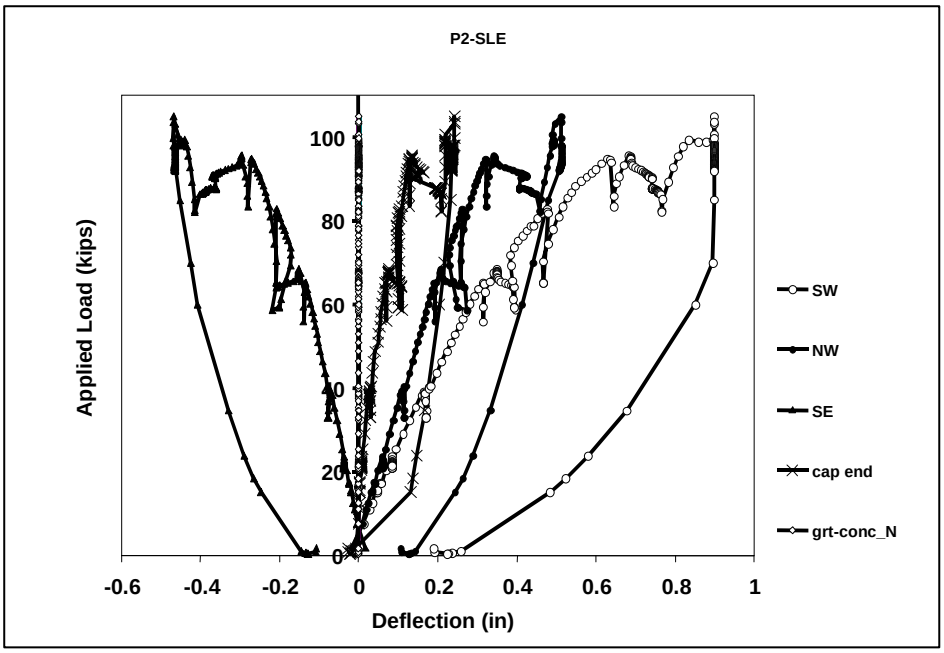

Figure 3.17 Load-deflection response for Test 6

3.3 CONCLUSION

The single line grout pocket connection behavior was acceptable under the service-level and ultimate-level loadings. It failed as expected by yielding of the connection anchorage bars near the bedding layer. During loading, flexural cracks were observed, as anticipated, in the beam cap. As loading eccentricities increased, the pile segment started to crack on the tension side. Crack widths on the cap and pile were under acceptable limits of 0.013 in.

The main issue raised by this test was the durability concerns associated with the exposed top surface of the grout pocket. It appeared to be very permeable. Later, coring of the pocket showed that the porous material extended 3 in. below the top surface.

Another issue was the grout strength. It is desirable that the grout strength be equal or higher than the concrete strength. On the test day, strengths of the concrete and grout were 5.6 ksi and 4.0 ksi, respectively. Although this was not advantageous, it did not result in adverse behavior such as slip or crushing of the grout.

The development length of 15 in. inside the cap was satisfactory. It behaved well under service-level loads and yielded before brittle failure occurred.

CHAPTER 4

RESULTS OF DOUBLE-LINE GROUT POCKET TESTS

4.1 INTRODUCTION

The double line grout pocket connection tests investigated the adequacy of a cast-in-place column and a precast cap connection. A double line of two epoxy-coated #9 straight bars with 15 in. embedment depth and Sika 212 grout were used in the connection. During grouting, a considerable amount of segregation was observed and associated problems with adequately filling the bedding layer by gravity flow grouting and the use of 0.5 in. vent tubes were experienced.

Four tests incorporating different loading conditions were conducted on the specimen. The load sequence shown in Table 4.1 was used to subject the connection to increasingly-severe load combinations.

Based on typical conditions for column bents, a maximum combined factored dead and live load of 290 kips was applied on each side of the connection, totaling 580 kips at the column top. These loads were typically applied with eccentricities in the 4 to 7 in. range. As shown in the photograph of the test setup of specimen C2-DL(Figure 4.1), vertical loads were applied to the cap using a total of four 100-ton rams, two on each side of the connection. In the load combinations shown below, the first three tests (1-3b) were considered to be proof loads for the connection. A very large transverse eccentricity of 55.5 in. in Test 4 was used to initiate yielding of connectors.

Table 4.1 Loading History

C2-DL Test No.	Eccentricity, e (in)		Applied Load (kips)		Notes
	Trans.	Long.	Vertical	Horizontal	
1	4.25	0	280	0	Proof load
2a	4.25	6	212 (service)	40	Proof load
2b	4.25	6	280 (ultimate)	40	Proof load
3a	7.25	6	209 (service)	40	Proof load (upper limit)
3b	7.25	6	280 (ultimate)	40	Proof load (upper limit)
4	55.5	0	To failure	0	Failure eccentricity; loaded one side only

Figure 4.1 Test setup

4.2 TEST RESULTS AND GENERAL BEHAVIOR

4.2.1 Test 1

Similar to the single-line specimen, the pre-existing cracks had been examined in the grout pockets and specimen were marked before the test was initiated. Only minor pre-existing cracks were observed on the pocket surfaces. However, the top of the pockets had a soft paste-like material that extended at least 2 in. deep. The bent cap also had pre-existing hairline cracks on both side faces which were due to the cap dead load moment and construction loads. During the post-grouting inspection of the specimen, a 0.25 in. wide gap on the south side of the bedding layer was observed. The gap was 2.5 in. wide and extended approximately 5.5 in. into the bedding layer. Segregation of the grout together with the location of the south shim may have caused this gap. The presence of the gap, however, did not affect structural performance, but such a gap may cause durability problems in the long term.

At the first load increment to 22 kips (applied to both cap ends) minor cracks with had widths less than 0.005 in. appeared in the grout. These may have been related primarily to the weak, paste-like grout on the surface. Flexural cracks appeared gradually as load was increased through 106 kips. At the full service load of 205 kips (each end), crack widths on the cap beam and pocket surfaces were 0.009 in. or less. Flexural cracks through the pocket did not adversely impact connection performance at this level.

The north side of specimen C2-DL is shown in Figure 4.2 at a load of 285 kips applied on each end, which was the factored load level for Test 1. Shear

cracks appeared and flexural cracks extended as the factored load was approached. Cracks widened to as large as 0.013 in. on the side faces of the cap and 0.009 in. on the pocket surfaces. Additional cracks appeared in the bedding layer. (Crack marks on the photograph were intentionally thickened to make them visible)

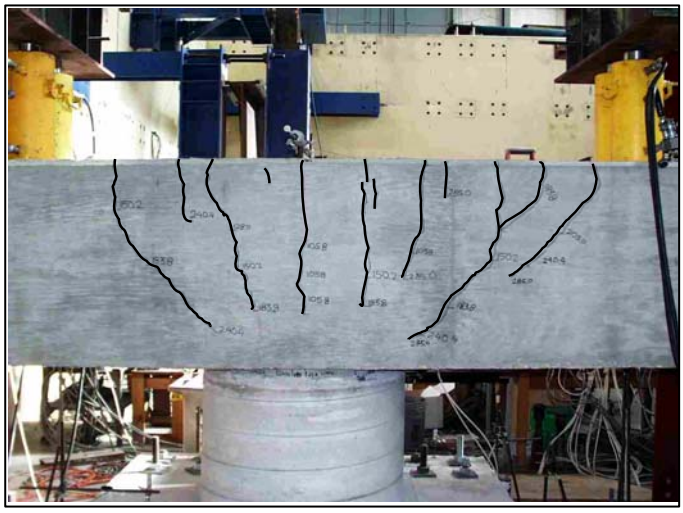

Figure 4.2 Cracks on north side of specimen C2-DL after Test 1

Load-strain and load-deflection plots for Test 1 are shown in Figures 4.3 and 4.4, respectively. Strain records confirmed that the connectors experienced very low levels of stress. Connectors remained essentially in compression throughout loading, and maximum strain levels were less than 20% of nominal yield. The maximum strain occurred in the southwest bar. Although there was no longitudinal eccentricity, the strain records were not the same for the connectors on the same end of the cap. This was likely due to the gap in the bedding layer which resulted in a shift in the neutral axis. Load-displacement response of the cap demonstrated some softening of the system as flexural cracks developed. The maximum measured displacement was less than 0.2 in. at the west tip of the cap beam. Grout-concrete relative displacements were zero.

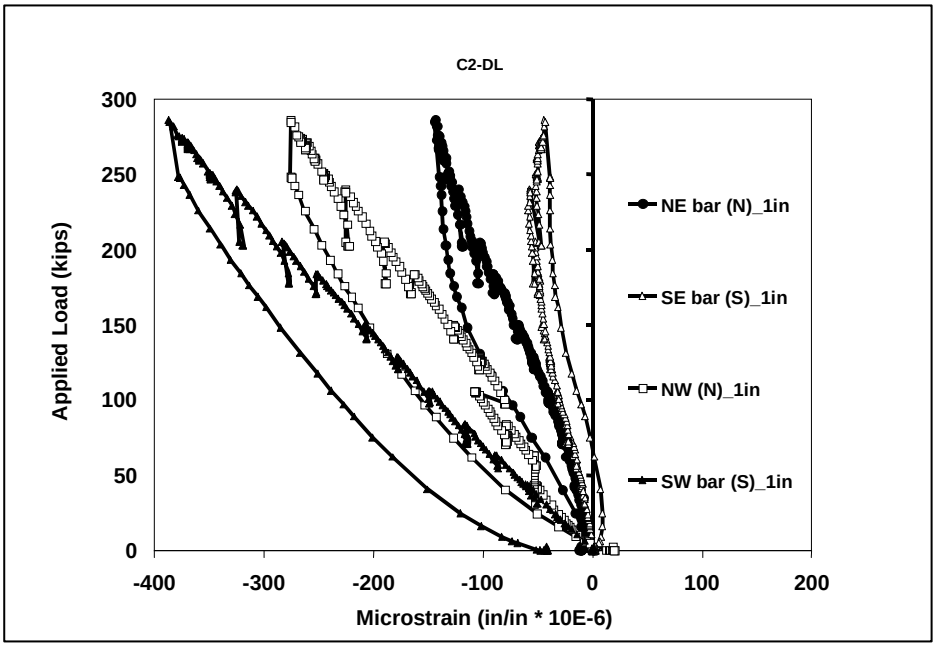

Figure 4.3 Load-strain response for Test 1

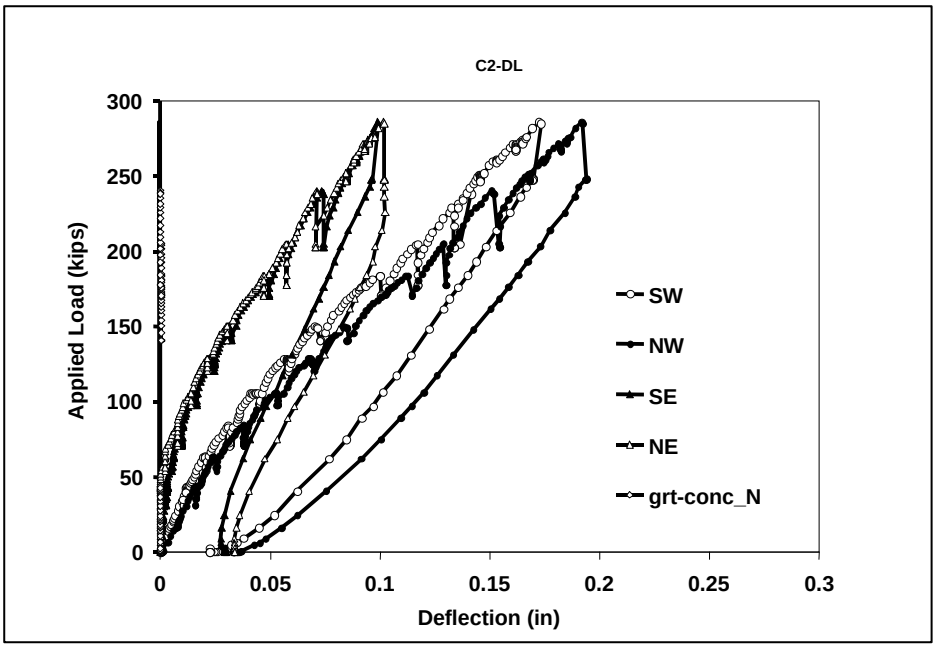

Figure 4.4 Load-deflection response for Test 1

4.2.2 Test 2

Pre-existing cracks reopened upon application of load. At the service level of 212 kips applied on each end, cracks extended on the side faces and new cracks appeared on the top of the cap. Maximum crack widths at the cap top and grout pockets were slightly larger than the crack widths in Test 1.

Unlike Test 1, a horizontal load of 40 kips was applied along the longitudinal axis of the cap at the service level load. This horizontal load did not cause formation of new cracks or measurable opening of existing cracks. However, it generated a 20% strain increase in the northeast connector bar and a 0.05 in. increase in horizontal deflection of the bent cap as shown in the strain and deflection responses for Test 2 in Figures 4.5 and 4.6, respectively.

At the factored load of 280 kips, new shear cracks appeared on the both sides of the cap beam. Flexural cracks extended as the factored load was approached. Existing flexural and shear cracks widened. Application of the horizontal load caused minor observable changes. Cracks in the pocket did not adversely impact connection performance.

In contrast to Test 1, strain records showed the north bars to be in tension with slightly less than 25% of nominal yield stress in the northeast bar. The maximum displacement at the west tip of the cap was 0.30 in., which was 50% greater than measured during Test 1. Grout-concrete relative displacements were negligible.

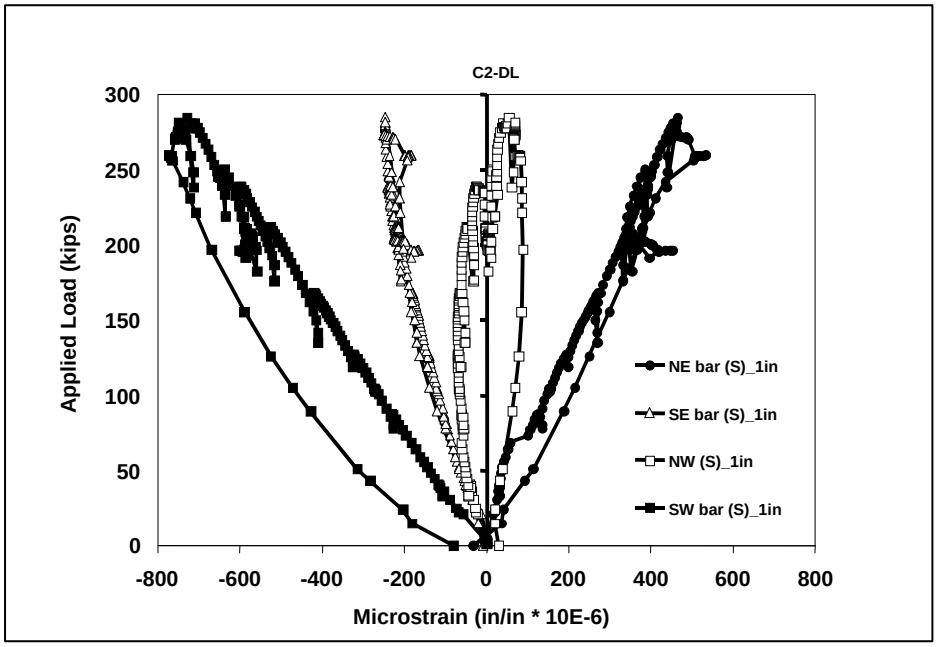

Figure 4.5 Load-strain response for Test 2

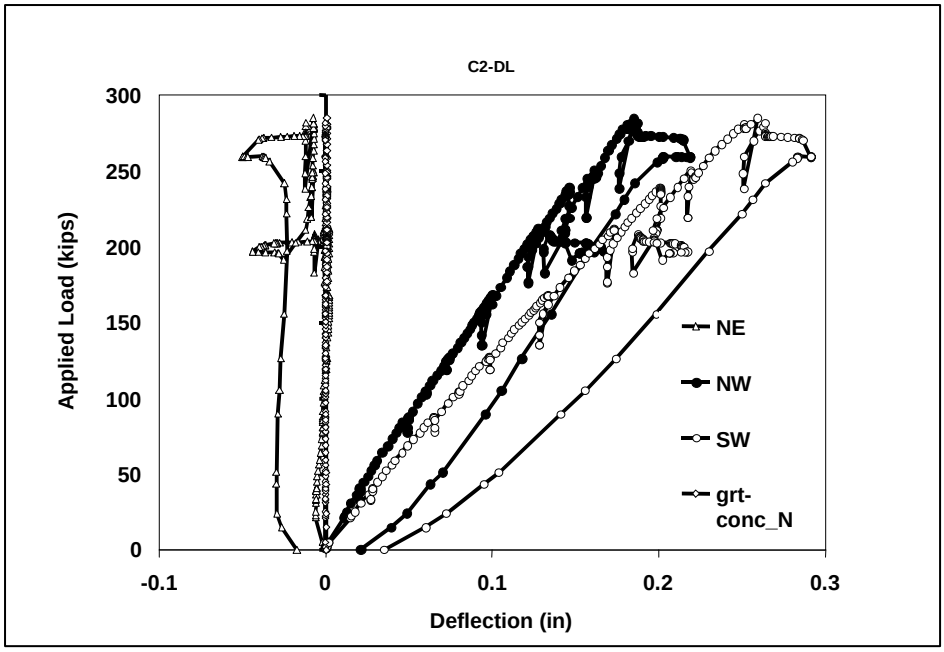

Figure 4.6 Load-deflection response for Test 2

4.2.3 Test 3

As an upper-limit proof load, the transverse eccentricity of the loads was increased to 7.25 in. and the longitudinal eccentricity was increased to 6 in. No visible difference in response was observed untill service level was reached, although instrument readings indicated much larger maximum strains in the connectors. Maximum crack widths matched those in Test 2. Load-strain plots (Figure 4.7) show the increase in bar strains that occurred as vertical and then horizontal loads were applied. The north bars were in tension, and the southwest bar was under compression at the service-level load. The southeast bar was vey near to the neutral axis at service level. A crack wrapping around ¼ of the column base appeared when the horizontal load of 40 kips was applied. Load-deflection plots (Figure 4.8) were linear up to service level, and the effect of horizontal load was slight.

At a load of 255 kips, a horizontal crack appeared on the northeast side of the column near mid-height, as shown in Figure 4.9. As load was increased to the factored load level, this crack extended in the column and new shear cracks appeared on the south face of the cap beam. Upon application of the horizontal load, vertical cracks appeared on the west column face, and the horizontal column crack and beam shear cracks extended. Maximum crack width at the pocket top was slightly larger than during Test 2. Grout-concrete relative displacements were still negligible as shown in the displacement response.

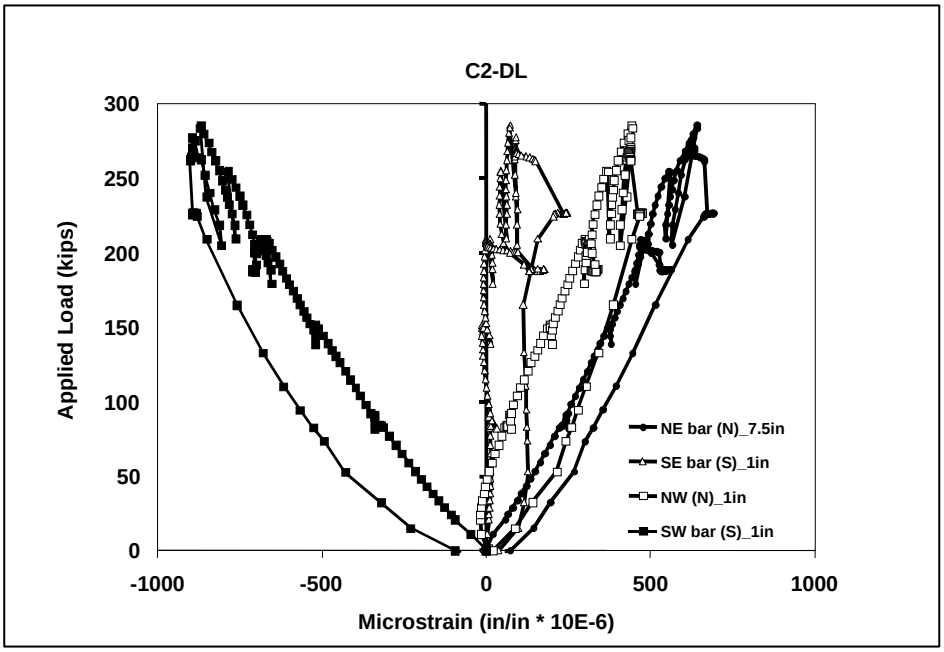

Figure 4.7 Load-strain response for Test 3

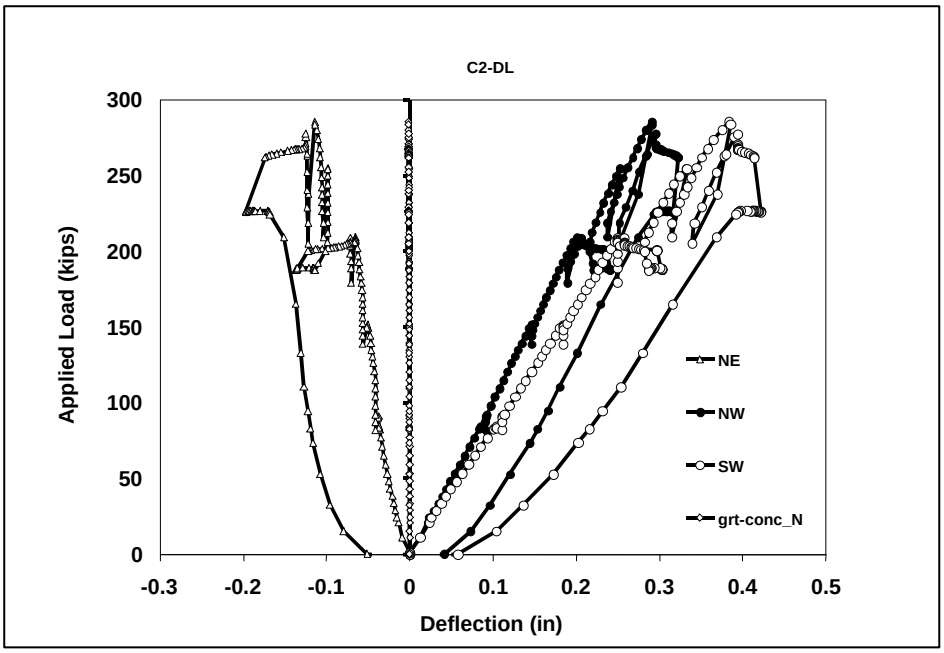

Figure 4.8 Load-deflection response for Test 3

Figure 4.9 Column cracks during Test 3

4.2.4 Test 4

In order to yield the connectors, a large transverse eccentricity of 55.5 in. was used by locating a single ram on the west end of the cap beam. At 33 kips, strain in the southeast connector reached approximately 67% of nominal yield as shown in the strain history for Test 4 (Figure 4.10). At this load the pre-existing column cracks wrapped around the east side of the column. At 47 kips, connector strains nearly reached yield and a new column crack appeared just below the bedding layer. This opening into the bedding layer occurred due to the shift in neutral axis toward the west side of the connection.

The load-strain plots show that at 60 kips the southeast connector yielded at 1 in. above the bedding layer. Load-deflection plots (Figure 4.11) clearly show

the change in stiffness corresponding to significant additional cracking on the tension (east) side of the column. Crack widths on the top surface of the grout pockets, which were a maximum of 0.016 in., did not widen further during the Test 4 loading. At approximately 80 kips, yielding occurred at 7.5 in. above the bedding layer in the northeast and southeast connectors. No additional cracks appeared on the side faces of the cap beam at this level. Test 4 demonstrated that a 15 in. embedment provided sufficient anchorage to yield the #9 connectors without observable distress in the connection.

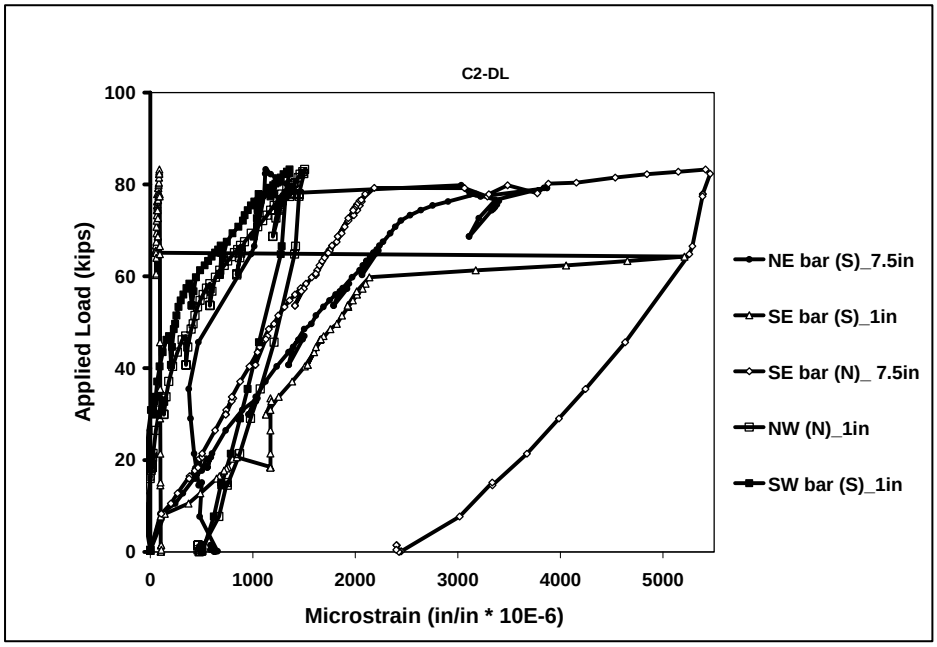

Figure 4.10 Load-strain response for Test 4

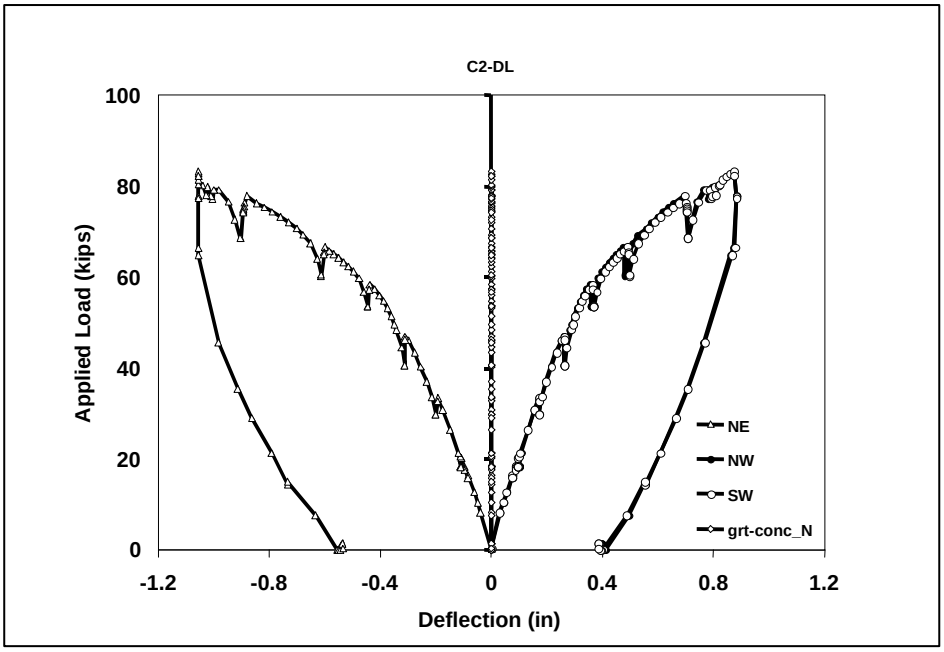

Figure 4.11 Load-deflection response for Test 4

4.3 CONCLUSION

Performance of the double-line grout pocket connection for the proof loads of Tests 1 through 3 was excellent. Adequate strength and stiffness were evident. Even during Test 3 with combined maximum eccentricities of 7.25 in. and 6 in. in the transverse and longitudinal directions, respectively, the connectors (including anchorages) were challenged very little. Maximum bar strains were less than half of nominal yield and there was no measurable slip between the pockets and cap beam. Test 4 proved that the grouted connections possessed sufficient anchorage at 15 in. embedment to yield the #9 connectors without causing observable distress in the connection. The use of steel shims in the bedding layer did not affect structural performance during testing. However, the presence of shims in the bedding layer during grouting, segregation of the grout, and use of a gravity flow system for grouting from the top of the pocket contributed to the formation of a gap at the south side of the bedding layer. Such a gap could pose durability concerns in the long term, and must be avoided in grouting of the connection.

CHAPTER 5

RESULTS OF VERTICAL DUCT TESTS

5.1 INTRODUCTION

The vertical duct connection tests investigated the adequacy of a cast-in-place column and precast cap connection. Straight, epoxy-coated #9 bars with a 15 in. embedment depth in each of four, 4 in. diameter steel corrugated ducts, and Masterflow 928 grout were used in the connection. In contrast to the first two specimens, grout used in specimen C2-VD had no previous history of problems in Phase I tests. Neither air nor bleed water was evident at the surface after grouting. The following day the top surfaces of the grout appeared smooth and at roughly the same elevation as the cap. Unlike the previous specimens, the surface of the bedding layer was completely filled with no evidence of gaps.

Four tests incorporating different loading conditions were conducted on the specimen. The load sequence shown in Table 5.1 was used to subject the connection to increasingly-severe load combinations.

Similar to the double-line specimen, a maximum combined factored dead and live load of 285 kips was applied on each side of the connection together with eccentricities in the 4 to 7 in. range. In the combinations shown below, the first three tests were considered proof loads for the connection. A very large transverse eccentricity was used in Test 4 to initiate yielding of the connectors. The test setup for specimen C2-VD was similar to that used for specimen C2-DL.

Two 100-ton rams on each side of the connection were used to apply the vertical loads.

Table 5.1 Loading History

C2-VD Test No.	Eccentricity, e (in)		Applied Load (kips)		Notes
	Trans.	Long.	Vertical	Horizontal	
1	4.25	0	285	0	Proof load
2a	4.25	6	202 (service)	40	Proof load
2b	4.25	6	282 (ultimate)	0	Proof load
3a	7	6	202 (service)	30	Proof load (upper limit)
3b	7	6	284 (ultimate)	40	Proof load (upper limit)
4	55.5	0	To failure	0	Failure eccentricity; loaded one side only

5.2 TEST RESULTS AND GENERAL BEHAVIOR

5.2.1 Test 1

Before testing was initiated, the specimen was examined for any cracks and irregularities. Hairline cracks were observed on the north and south side of the bedding layer. These likely occurred due to shrinkage. Additionally, there few pre-existing cracks on the cap beam as a result of dead load moments and construction loads were observed. Moreover, the specimen was contained some imperfections it the column-and-footing segment. The column was became inclined approximately two degrees in the north direction during concrete casting

as the result of inadequate bracing of the formwork. In addition, the base of the footing was not flat because the plywood used to form the base was sagged between 2 x 4's used to support it.

New flexural cracks were observed at 85 kips applied to each cap end. The cracks started adjacent to ducts and extended through the edges of the beam. The load was 63 kips applied to each end when flexural cracking was observed in the C2-DL specimen during Test 1. As load was increased, the cracks widened. New cracks were observed at 107 kips, and they extended down on the side faces about 1/3 the beam depth. These cracks did not spread through the grout inside the ducts. The steel ducts arrested cracks. At the full service-level load of 205 kips, additional shear cracks on the sides and flexural cracks on top of the cap beam were observed. Crack widths were less than 0.007 in. No cracking was observed in the bedding layer at service load.

At factored load (285 kips each side) new cracks were observed close to the rams, and the existing cracks extended down the sides of the cap. The maximum crack width measured at this level was 0.007 in. Figure 5.1 shows the cracks marked on the north side of the cap beam after Test 1 (crack marks on the photograph were intentionally thickened to make them visible).

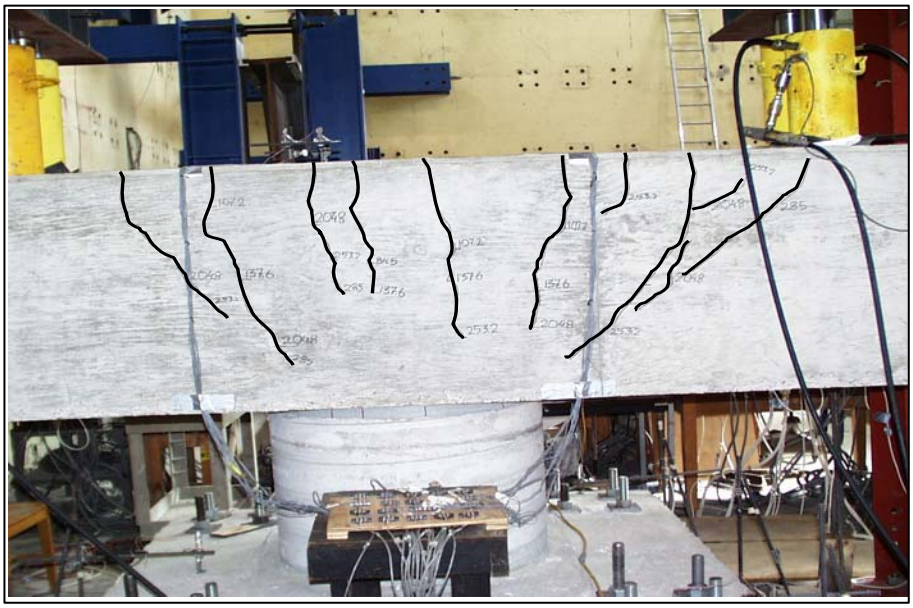

Figure 5.1 North side of specimen C2-VD after Test 1

Strain and deflection responses for the vertical duct specimen are shown in Figures 5.2 and 5.3, respectively. Instrument readings confirmed that the connectors sustained very low levels of stress. Strains in the west connectors at 1 in. above the bedding layer were the same due to zero longitudinal eccentricity. However, there were minor differences in strains for the east connectors. The Connectors remained essentially in compression throughout loading, and maximum strain levels were less than 10% of nominal yield which was approximately half the strains measured in the double-line specimen during Test 1. Measured duct strains were very low. The Load-displacement response of the cap demonstrated some softening of the system as flexural cracking developed at 85 kips. The maximum tip deflection of 0.2 in. at the west end of the cap beam

was the same as for specimen C2-DL during Test 1. Grout slip inside the steel ducts was negligible.

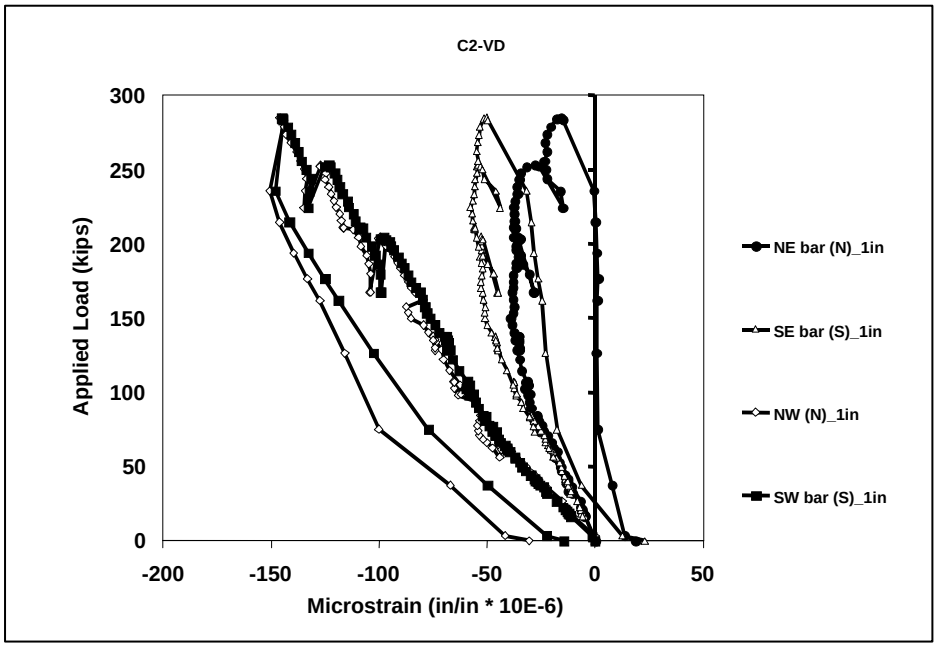

Figure 5.2 Load-strain response for Test 1

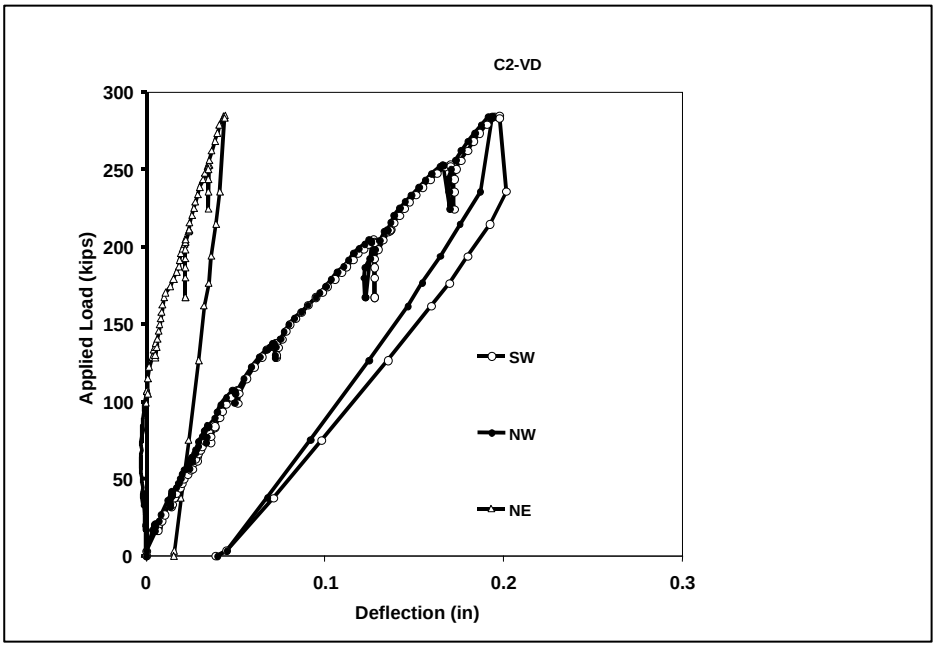

Figure 5.3 Load-deflection response for Test 1

5.2.2 TEST 2

Pre-existing cracks opened upon reloading. The north connectors were in tension during Test 2. At the service level of 202 kips applied to both endds, cracks formed in the footing with a maximum width of 0.007 in. There were no cracks at the grout surface.

A horizontal load of 40 kips was applied in the transverse (east-west) direction at the service level load. This load caused the footing cracks to widen to 0.013 in. and extend toward the south side. New vertical cracks formed in the bedding layer due to the horizontal loading. Records showed a 0.03 in. increase (40%) in horizontal deflection.

As the factored-load level of 282 kips was reached, new shear and flexural cracks formed at both sides of the cap beam. Cracks on top of the cap still did not spread into the grout inside the ducts. Cracks around the ducts during loading did not adversely impact connection performance. At this load the maximum crack width in the footing was 0.016 in.

Figures 5.4 and 5.5 show the strain and deflection responses for specimen C2-VD during Test 2. Strain records indicate that the northeast and northwest bars reached 20% and 15% of nominal yield, respectively. The maximum displacement at the west tip of the cap was approximately 0.29 in., which was 50% greater than the corresponding displacement in Test 1. It was noted that the footing experienced uplift during the test and this contributed to higher tip deflections compared to those in the double-line specimen during Test 2. This also resulted in a softer load-displacement response of the cap than during Test 1. Grout slip inside the ducts was negligible.

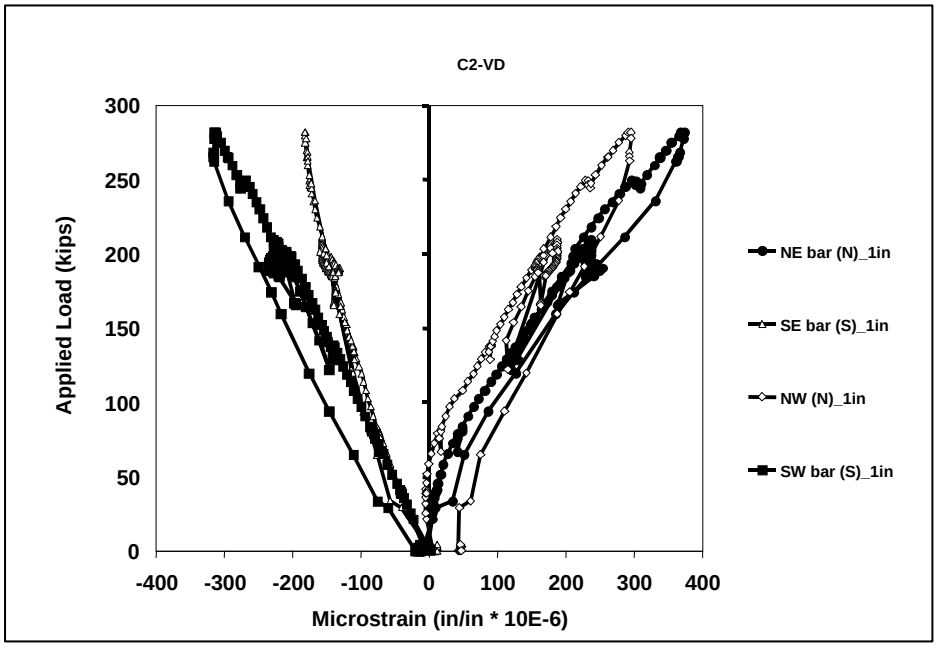

Figure 5.4 Load-strain response for Test 2

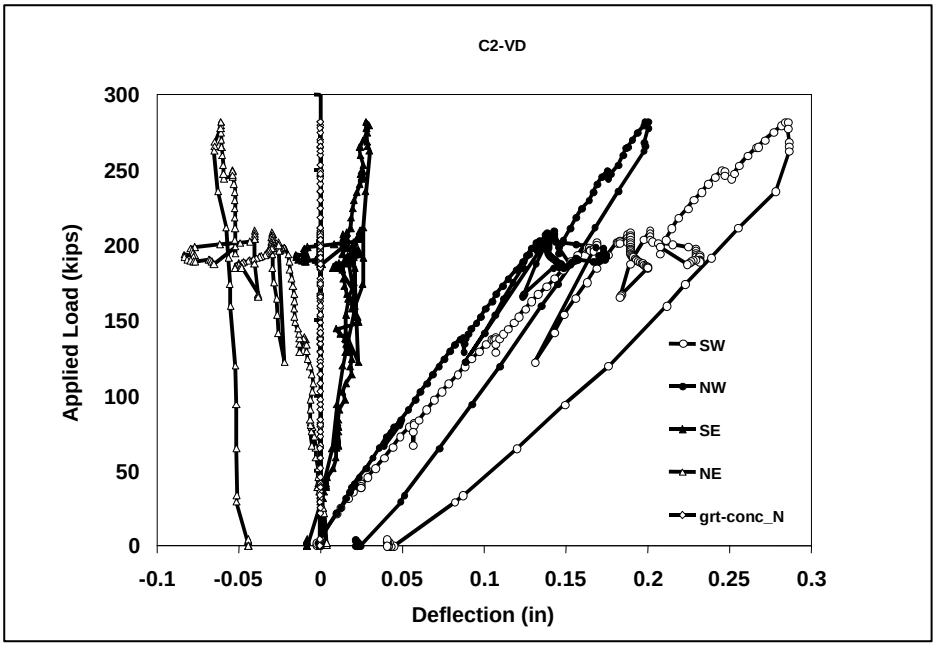

Figure 5.5 Load-deflection response for Test 2

5.2.3 Test 3

For Test 3, the transverse eccentricity was increased to 7 in. as an upper-limit proof test for the vertical duct connection. At service level, the maximum tensile strain on the connectors was less than 20% of nominal yield. The crack widths on the cap were approximately 0.005 to 0.007 in. and were less than 0.013 in. With the application of a horizontal load of 30 kips, the cracks widened and extended. The transverse displacement of the cap increased by 0.02 in.

At the maximum factored load of 284 kips, a small opening was formed at the east side of the column-and-cap interface. There was still no indication of cracking on the grout top surface. Footing crack widths increased to 0.025 in. With the application of a horizontal force of 40 kips, deflections and strains were increased slightly.

Strain and deflection responses for Test 3 are shown in Figures 5.6 and 5.7, respectively. The maximum strain at 1 in. above the bedding layer was less than 30% of nominal yield. The north connectors were again in tension as they were during Test 2. The southeast connector was very close to the neutral axis. The effect of the horizontal force was a small increase in strain at 1 in. above the bedding layer. The maximum tip deflection at the west end of the bent-cap was 0.37 in. Horizontal force caused a 75% increase in tip deflection at the northeast tip. It was observed that the horizontal force had more effect at the factored-load level than at the service-level loading. Grout slip inside the duct was negligible.

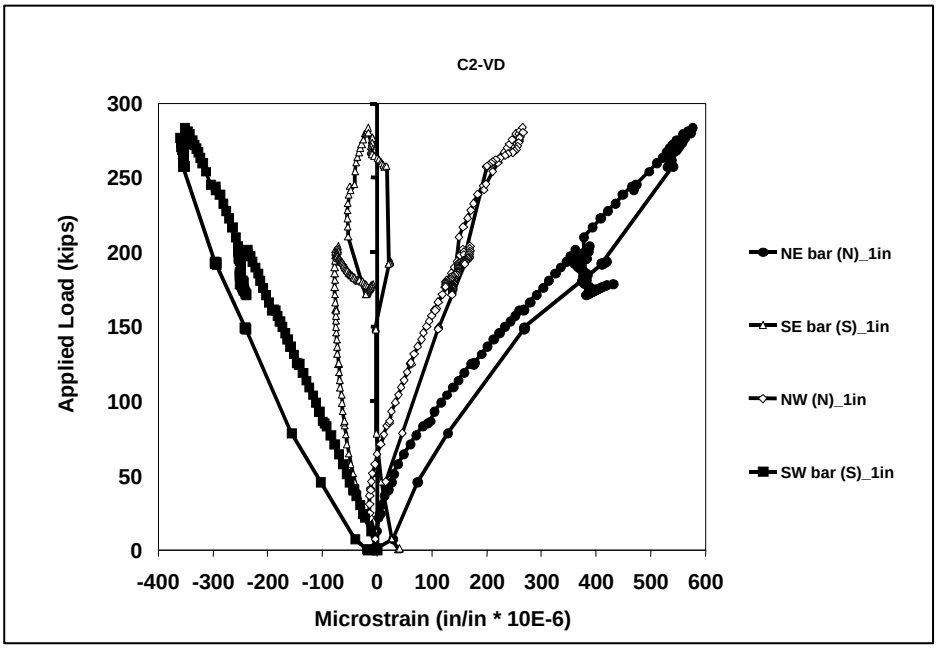

Figure 5.6 Load-strain response for Test 3

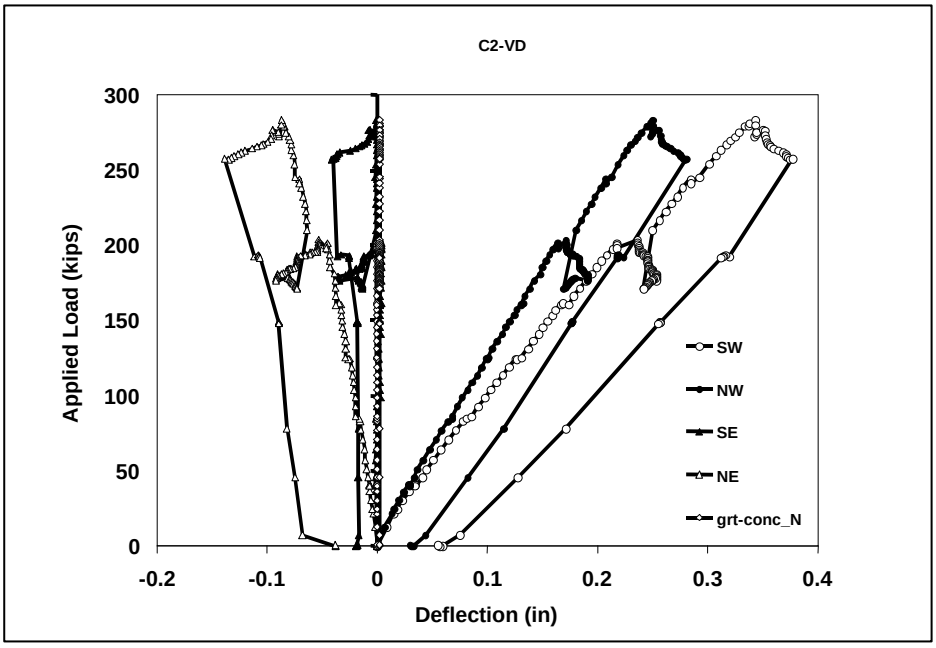

Figure5.7 Load-deflection response for Test 3

5.2.4 Test 4

The transverse eccentricity was increased to 55.5 in. by locating a single ram on the west end of the connection in order to test the anchorage of the connectors. At 26 kips, a horizontal crack formed at the east side of bedding layer.

New cracks appeared on the northwest and southwest sides of the cap at 61 kips. The southeast bar yielded first at 75 kips. At this level, new vertical and horizontal cracks formed at the column base and cracks at the column-footing interface extended on the south side. Even at this level of loading no cracks were observed on the top of the grout ducts.

As load was increased, the gap between the cap and column widened and caused the neutral axis to shift sigificantly. Despite of the high level of loading, behavior of grout in the vertical ducts was excellent. Figures 5.8 and 5.9 show the strain and deflection plots, respectively, for the C2-VD specimen during Test 4. At approximately 65 kips, the southeast connector bar yielded 1 in. above the bedding layer. As load was increased, some strain gages failed. The deflection plots revealed that these were not an indication of grout slip inside the ducts. The maximum deflection of the west tip was 0.95 in.

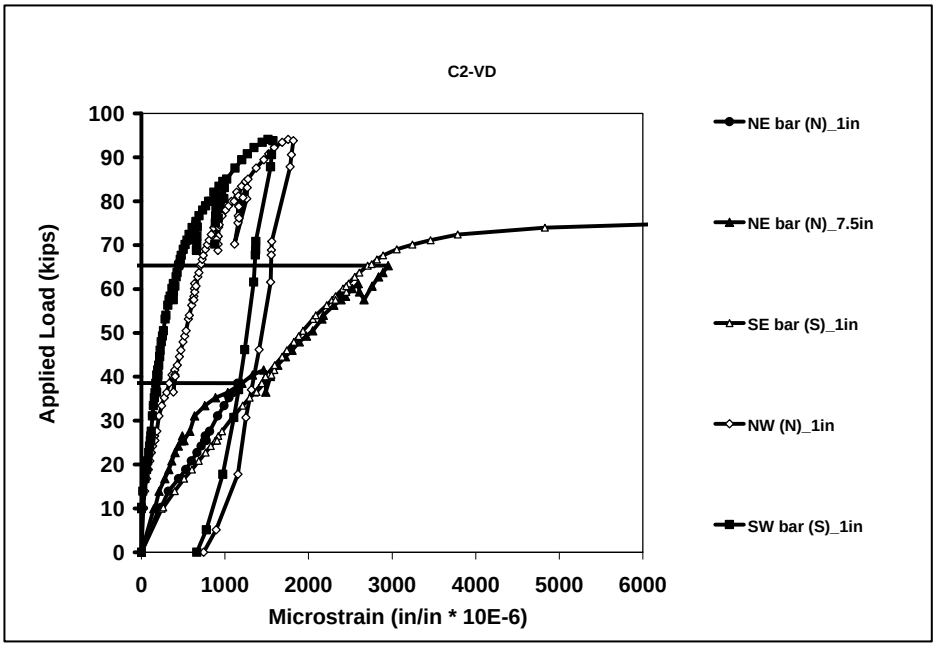

Figure 5.8 Load-strain response for Test 4

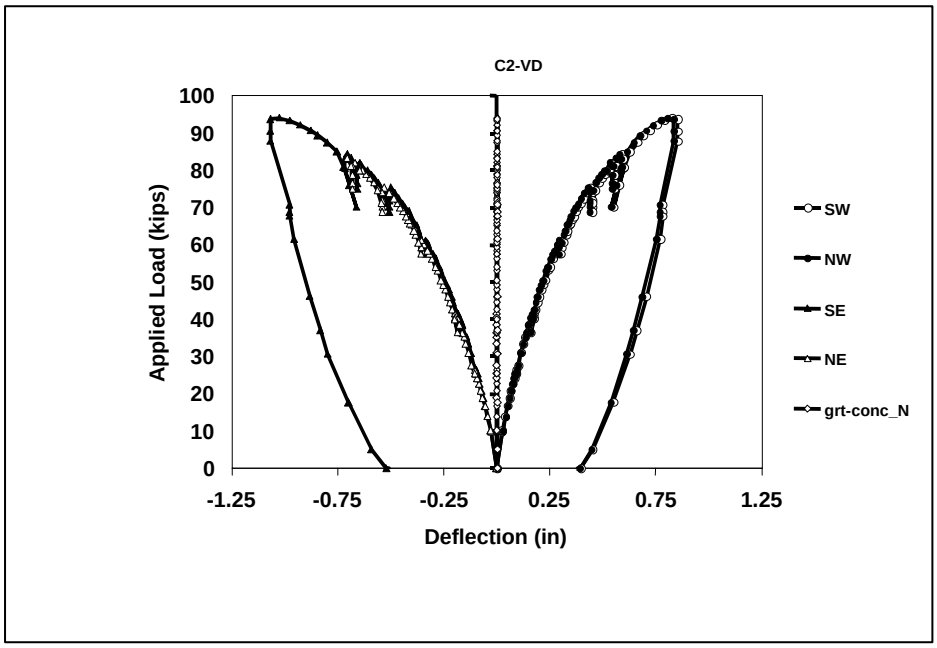

Figure 5.9 Load-deflection response for Test 4

5.3 CONCLUSION

Vertical duct connection performance was excellent. This specimen demonstrated better performance than the double-line specimen, having lower strains under similar loading conditions. During the proof tests, the connectors exhibited no distress with maximum bar strains less than 40% of nominal yield during Test 3. The 15 in. anchorage in vertical steel ducts was sufficient to yield the #9 connectors during Test 4. The usage of steel corrugated ducts served as a crack arrester to avoid extension of cracks into the grout. For this reason ducts are preferable to pocket connections detail. Compared with other grouts, Masterflow 928 had superior placement and in-situ performance.

CHAPTER 6

RESULTS OF BOLTED CONNECTION TESTS

6.1 INTRODUCTION

The adequacy of a cast-in-place column and precast cap connection using four 3-in. diameter steel corrugated ducts each with a 1 in. diameter threaded rod grouted inside the duct and secured on top of the cap with a nut was investigated. Masterflow 928 was again used for grouting the C2-BC specimen. In contrast to the vertical-duct specimen, entrapped air was observed adjacent to the rods after completing the grouting operation. During Phase 2 grouting, air appeared in the grout near the top surface only for grouts with longer flow durations (Single Line Pocket, Euclid High Flow, 53 sec; Bolted Connection, MF928, 53 sec), but not for shorter flows (Double Line Pocket, Sika 212, 17 sec; Vertical Duct, MF928, 34 sec). Based on Phase I tests, usually 30 seconds of flow is desirable.

Four tests incorporating different eccentricities and loading conditions were conducted on the specimen. The load sequence shown in Table 6.1 was used to subject the to connection increasingly-severe load combinations.

Similarly to other column-type specimens, a maximum combined factored dead and live load of 290 kips was applied at each loading point together with eccentricities in the 4 to 7 in. range. The first three tests were proof tests, and the last, Test 4, was intended to push the connectors well into the nonlinear range of

response. The test setup had two 100-ton rams on each side of the connection, as in the two previous tests.

Table 6.1 Loading History

C2-BC Test	Eccentricity, e (in)		Applied Load (kips)		Notes
	Trans.	Long.	Vertical	Horizontal	
1	4.25	0	285	0	Proof load
2a	4.25	6	209 (service)	38	Proof load
2b	4.25	6	282 (ultimate)	0	Proof load
3a	7	6	202 (service)	40	Proof load (upper limit)
3b	7	6	285 (ultimate)	40	Proof load (upper limit)
4	55.5	0	To failure	0	Failure eccentricity; loaded one side only

6.2 TEST RESULTS AND GENERAL BEHAVIOR

6.2.1 Test 1

Before testing began, bolts were tightened to 200 lb-ft with a torque wrench as shown in Figure 6.1. A portion of each circular washer was cut away so that the strain gage lead wires exiting the top of the grouted ducts were not crushed while tightening the nuts. During the usual examination of the specimen before testing, some cracks were observed in the footing.

Figure 6.1 Tightening nuts on top of cap

The first flexural cracks were noted at 85 kips applied to both ends of the cap, which was the same as for the vertical-duct specimen. These cracks extended mostly down the side faces of the cap beam as load was increased to 127 kips. At the service-level load of 201 kips, the maximum crack width was 0.007 in. on the side faces and cap beam top. Because the top of each grout surface was covered with a nut and washer, it was impossible to observe the grout surface.

At factored-level of loads (285 kips each side) extension of shear cracks on the side faces and flexural cracks on top of the cap beam was observed. Figure 6.2 shows the north side of specimen C2-BC after Test 1. The maximum width of

the cracks was less than 0.007 in. at factored loads. (The crack marks on the photograph were intentionally thickened to make them visible.)

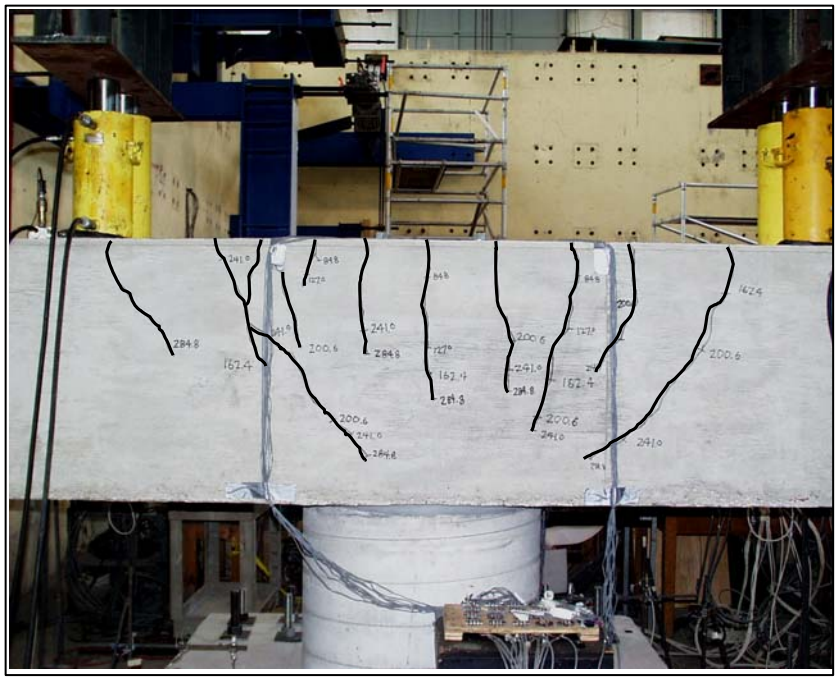

Figure 6.2 North side of the specimen C2-BC after Test 1

Figures 6.3 and 6.4 are the load-strain and load-deflection plots for the bolted connection response during Test 1, respectively. Strains on the east bars at 1 in. above the bedding layer started first in compression and then turned to tension beyond service level load. Strains at 7.5 in. confirmed the strains at 1 in. Connectors sustained very low levels of strain, which were less than 10% of yield. In contrast to other column-type specimens, the tip deflection of the cap exceeded 0.20 in., which was slightly higher than the deflections of other column-type specimens during Test 1. Measured strains on ducts were very low.

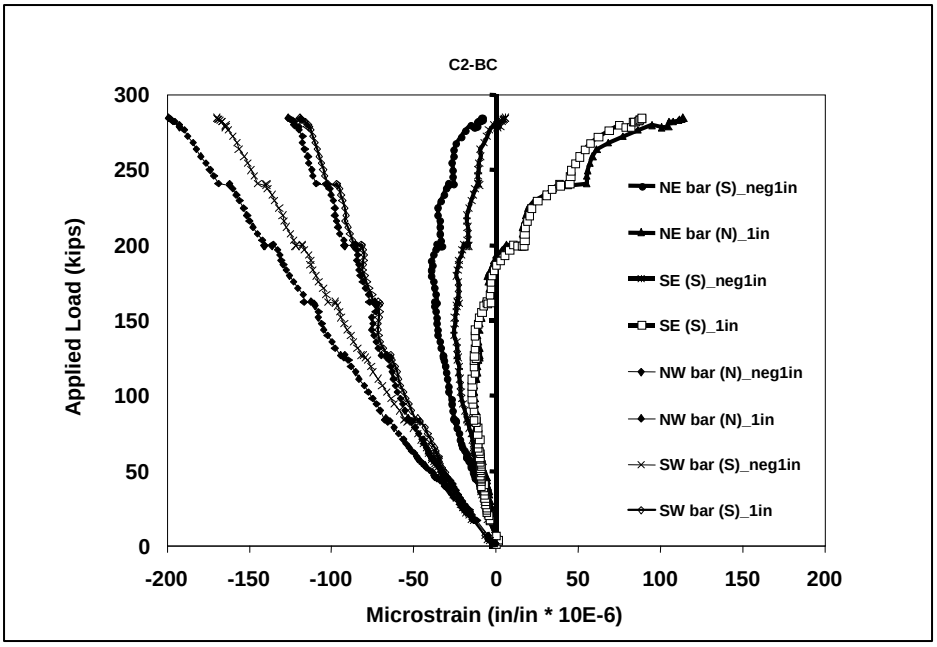

Figure 6.3 Load-strain response for Test 1

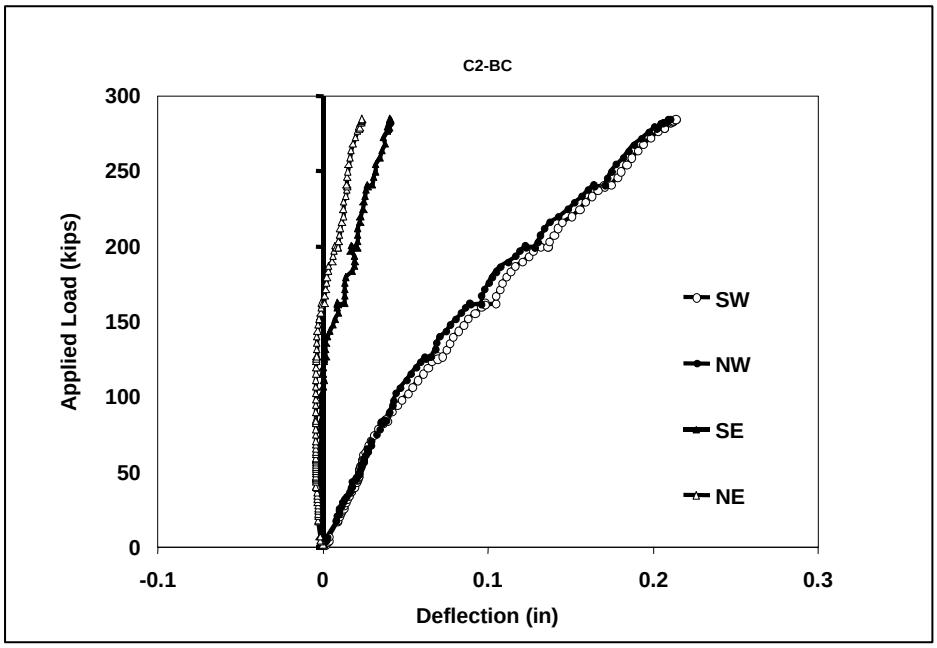

Figure 6.4 Load-deflection response for Test 1

6.2.2 Test 2

The behavior of the bolted connection was very similar to behavior of the vertical-duct specimen during Test 2. Up to 82 kips applied each end of the cap, nothing new was observed. Pre-existing cracks reopened. As load was increased to 126 kips, the crack at the east side of the footing was 0.0013 in. wide. At the service level of 209 kips applied at both cap ends, a horizontal force of 38 kips was applied. Strain responses (Figure 6.5), show that the north connectors were in tension at 1 in. above the bedding layer, and the south connectors were under compression. As shown in the load-deflection plots (Figure 6.6), horizontal load did not significantly affect the tip deflections at service level.

After the horizontal force was released, the vertical load was increased to 286 kips. New shear and flexural cracks appeared during this increment. At this level, a horizontal force of 40 kips was applied again. This caused the northeast connector bar stain to increase slightly. Strain records indicate that maximum strain was approximately 18% of yield at 1 in. above the bedding layer. This strain was slightly higher than the strain at 1 in. above the bedding layer in the vertical-duct specimen, which was approximately 20% of nominal yield in Test 2. The load-deflection response of the cracked section was linear and the maximum displacement, which occurred at the southwest tip, was 0.27 in.

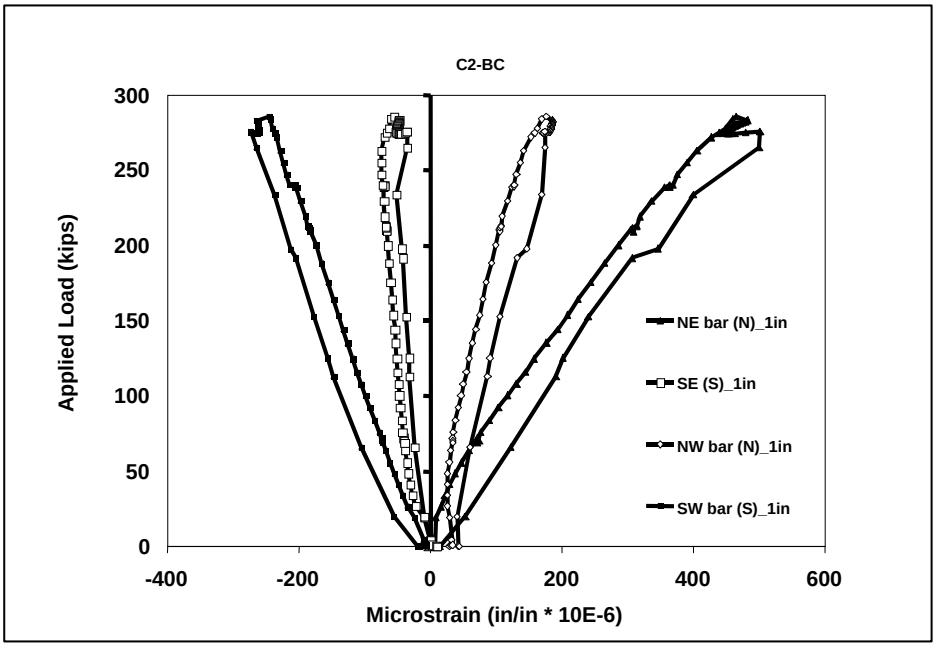

Figure 6.5 Load-strain response for Test 2

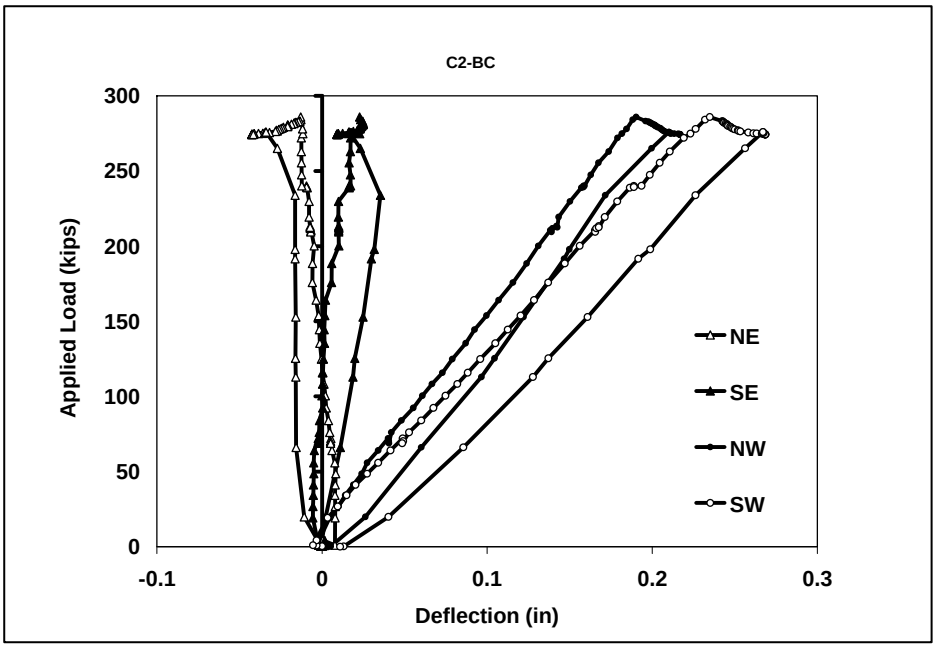

Figure 6.6 Load-deflection response for Test 2

6.2.3 Test 3

As an upper-limit proof load, the transverse eccentricity was increased to 7 in. for Test 3. Up to the service-level load of 202 kips at each end, nothing new was observed but the reopening of existing cracks. The strain and deflection responses for Test 3 are shown in Figures 6.7 and 6.8, respectively. With the application of a 40-kip horizontal force, tip deflections increased at both ends of the cap beam.

At 243 kips new cracks appeared on the top of the cap and new shear cracks formed on the south face.

The maximum load applied to the specimen was 285 kips. Instrument readings indicate that the maximum strain was less than 25% of yield. The load-deflection response was linear and the southwest tip deflected 0.36 in. at factored load.

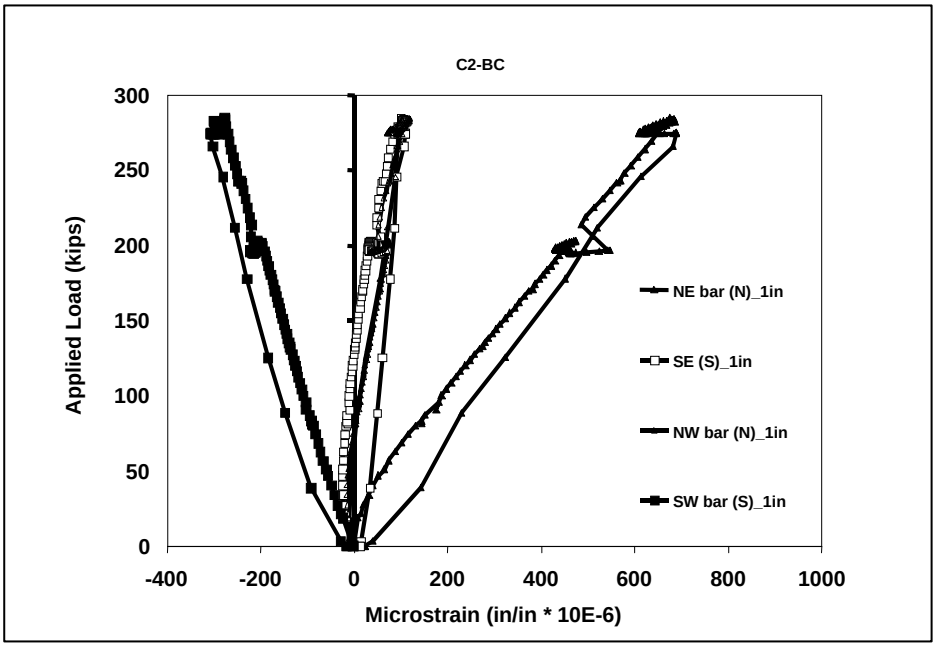

Figure 6.7 Load-strain response for Test 3

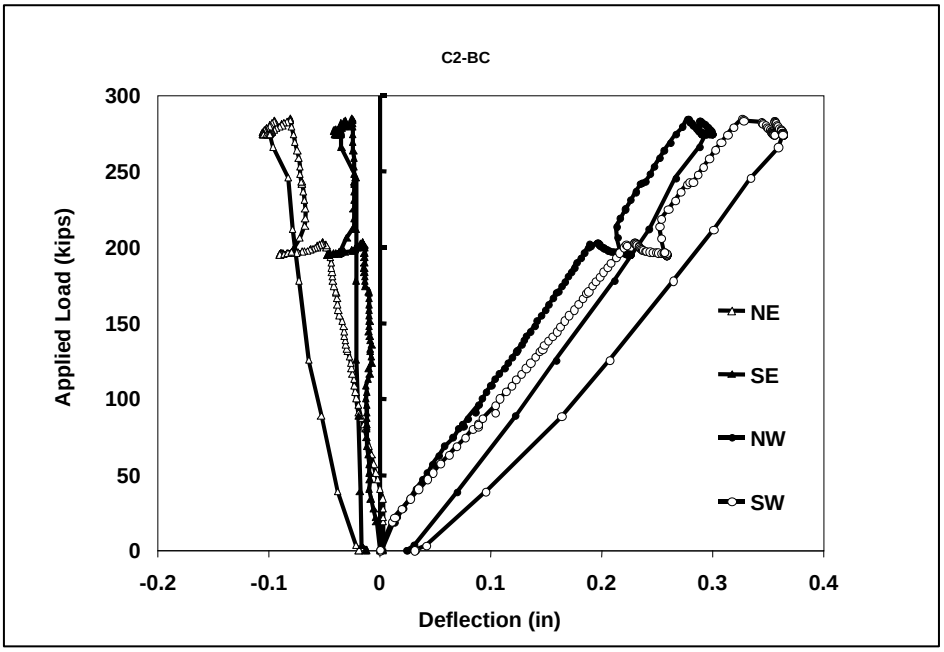

Figure 6.8 Load-deflection response for Test 3

6.2.4 Test 4

The transverse eccentricity was increased to 55.5 in. by locating a single ram at the west end of the connection, to test the threaded connecting bars. At a very low-level load of 26 kips, all strains at 1 in. above the bedding layer were in tension. As load was increased, cracks opened at the southeast side of the bedding layer, shifting the neutral axis toward the west side. It also caused more cracking in the column face. The maximum load applied to the connection was 87.5 kips. At this level there was visible concrete crushing on the west side of the column.

Load-strain and load-deformation plots are shown in Figures 6.9 and 6.10, respectively. The strain responses measured at 1in. above and 1 in. below the bedding layer were approximately for nearly all the connectors. The load-deflection curve showed gradual softening as load was increased.

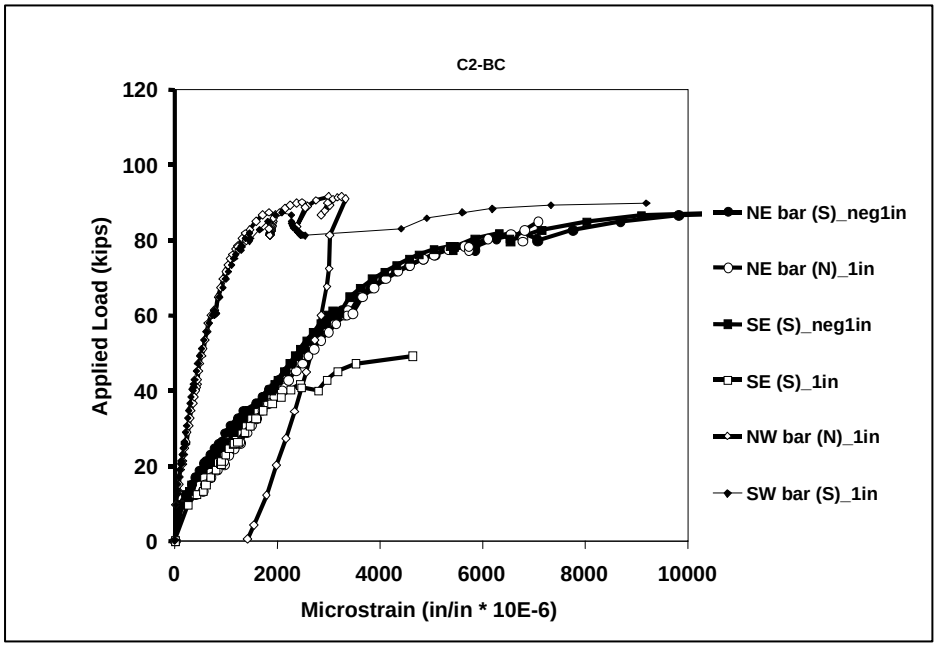

Figure 6.9 Load-strain response for Test 4

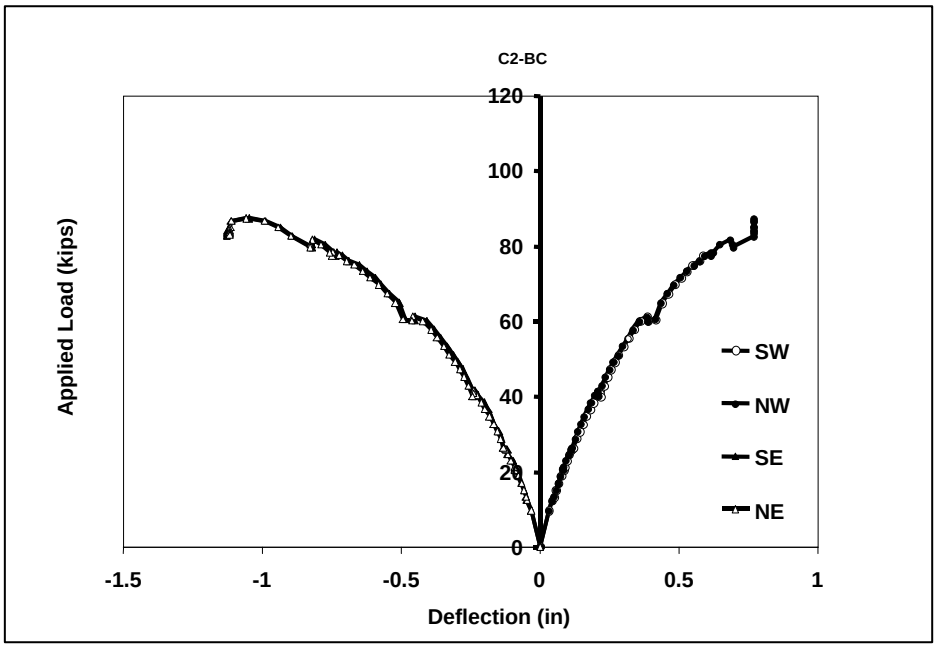

Figure 6.10 Load-deflection response for Test 4

6.3 CONCLUSION

The bolted connection detail performed quite well. Connectors were not loaded beyond approximately 25% of yield during the proof loads of Tests 1 through 3b. Under the unrealistic loading of Test 4, the threaded rods yielded. Three-in. diameter steel corrugated ducts were used in specimen C2-BC, which made the grouting operation difficult. A minimum 4 in. diameter is suggested for the ducts. It is also worth mentioning that during Phase 2 grouting, air near the top surface of the grout was observed for grouts with longer flow durations (Single Line Pocket, Euclid High Flow, 53 sec; Bolted Connection, MF928, 53 sec), but not for shorter flows (Double Line Pocket, Sika 212, 17 sec; Vertical Duct, MF928, 34 sec). Air in the grout might be due to one or more of the following: 1) longer flow time (due in part to a high temperature) corresponding to a thicker grout, resulting in slower rise of air through the grout after grouting and tamping; 2) extension of the rods to top of the duct, facilitating the path for air bubbles to the surface; and 3) movement of the lead wires to the edge of the rods after grouting. Based on Phase 2 results, a 20 to 40 second flow is recommended for a grout to minimize entrapped air. In addition, the use of a sealant at the top of the pocket is recommended.

CHAPTER 7

SUMMARY AND CONCLUSIONS

7.1 SUMMARY

Previous bridge construction projects in Texas demonstrated that precast bent-cap systems can result in savings of time and money. However, some issues related to economics, constructability, durability, and load transfer remained to be addressed. The Texas Department of Transportation, through the Center for Transportation Research at the University of Texas at Austin, funded a research program to investigate the development of connection details for precast bent-caps.

Four specimens with different connection details were tested in order to fully understand the behavior of connections, to examine constructability of connections, and to test preliminary design provisions developed in Phase I and used to proportion and detail of connections. Each specimen was subjected to a series of tests to progressively load the connections to more severe load combinations. Following is an overview of observations during the construction process and key results from the tests.

7.2 OVERVIEW OF OBSERVATIONS

During the construction of specimens, three different grout brands were used: Euclid Hi-Flow, Sika 212 and Masterflow 928. Only Euclid Hi-Flow had a lower compressive strength on test day than the concrete used in the specimen. No slip or crushing of grout occurred during testing despite the lower strength. In addition, it is important to mention that during Phase II grouting, air appeared at the surface of the grout only for grouts with longer flow times. Porosity in the surface of the grout suggests long-term durability problems. It is recommended that a trial batch of grout be mixed to test the flow rate before actual grouting.

The caps were designed to preclude flexural and shear or torsion failure. The expected failure modes were 1) anchorage failure in the pocket or duct, 2) concrete breakout around the pockets, and 3) concrete crushing at the column/cap interface. During proof tests to factored loads, no sign of distress was detected in any of the connections, deflections were reasonable, maximum stress in connecting bars was less than 30% of yield, grout/concrete relative slips were negligible, and corrugated steel ducts experienced low strains. Shear and flexural cracks in the bent-caps and columns or pile were less than 0.013 inches. To investigate the strength of each connection, unrealistic loading combinations were applied to each specimen. The precast connection bars yielded in each specimen. This was the desired connection failure.

7.3 CONCLUSIONS

The Phase II tests demonstrated that all four precast bent-cap connection specimens: the single-line grout pocket, double-line grout pocket, vertical-duct and bolted connections behaved as intended. Connections behaved elastically during service and factored-load tests, and strength of all connections was controlled by yielding of connection bars.

7.4 RECOMMENDATIONS FOR FUTURE RESEARCH

Precast connections were proportioned so anchorage of connecting bars between the column (or pile) and cap did not fail or yield under factored load conditions. The same cannot necessarily be said for cast-in-place bent-column connections used in current designs. Comparison of precast connection behavior with cast-in-place behavior would add additional perspective to the test results from Phase II. Long-term durability tests should be performed on exposed grout pockets to evaluate the ability of the grout to protect the connecting bars between the precast bent-cap and cast-in-place column or precast pile.

REFERENCE

1. LoBouno, Armstrong, & Associates, "Development of Precast Bridge Substructures," Research Report for the Florida Department of Transportation, May 1996.

2. Wolf, Lloyd M. and Friedman, Norman K., "Redfish Bay and Morris & Cummings Cut: Innovations in Bridge Construction and Durability," *Technical Quarterly*, V. 9, No. 2, October 1994, Texas Department of Transportation, Austin, pp. 1-3.

3. Waggoner, Mark C., " Reinforcement Anchorage in Grouted Connections for Precast Bridge Bent Cap Systems," M.S. Thesis, The University of Texas at Austin, May 1999.

4. Matsumoto, Eric E.; "Development of a Precast Bent Cap System," Ph.D Dissertation, The University of Texas, in process

5. Matsumoto, Eric E.; Waggoner, Mark C.; and Kreger, Michael E, "Development of Precast Bent Cap Systems and Testing Program," *Interim Report 1748-1*, Center for Transportation Research, The University of Texas at Austin, March 1998.

6. American Association of State Highway and Transportation Officials (AASHTO), *Standard Specifications for Highway Bridges*, 16th ed., AASHTO, Washington, D.C., 1992.

7. American Association of State Highway and Transportation Officials (AASHTO), *AASHTO LRFD Bridge Design Specifications: Customary U.S. Units*, 2nd ed., AASHTO, Washington, D.C., 1994.

8. ACI Committee 318, "Building Code Requirements for Structural Concrete and Commentary," *ACI 318-95/ACI 318R-95*, American Concrete Institute, Detroit, 1995.